OKLAHOMA GEOLOGY Notes

April 1998
Vol. 58, No. 2

On The Cover —

Small-Scale Duplex in the Arkansas Novaculite, Central Potato Hills, Ouachita Mountains

The cover photograph shows a small-scale duplex in the Arkansas Novaculite, exposed in Cedar Creek, Potato Hills (NW¼NW¼ sec. 31, T. 3 N., R. 20 E.). The view is vertical; stratigraphic up is to the north (top of photograph). The strata are oriented N. 78° W., 72° N. and are exposed on the south flank of an overturned anticline associated with the Cedar Creek thrust (~0.25 mi to the north). The main fault branches at the lower right. One branch continues directly up section; the other follows a bedding plane before it cuts up section (bottom center). The two branches rejoin near the left edge of the photograph. (Pocket knife is ~6 in. long.)

Mark W. Allen
EnecoTech, Inc.
Tulsa, Oklahoma

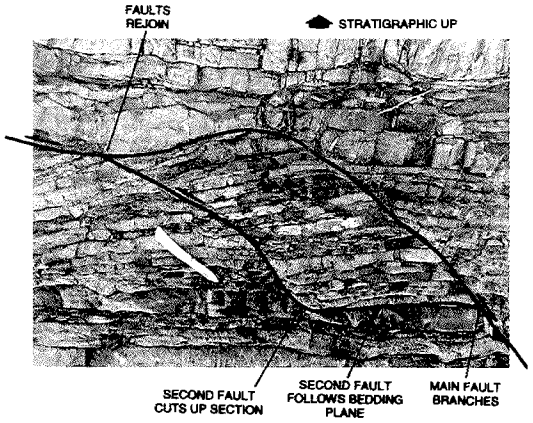

OKLAHOMA GEOLOGICAL SURVEY

CHARLES J. MANKIN
Director

KENNETH S. JOHNSON
Associate Director

OKLAHOMA GEOLOGY NOTES

Editor
Christie Cooper

Associate Editor
Tracy Peeters

Cartography
T. Wayne Furr, *Manager*
James H. Anderson
Charlotte Lloyd

OKLAHOMA GEOLOGY NOTES, ISSN 0030-1736, is published bimonthly by the Oklahoma Geological Survey. It contains short technical articles, mineral-industry and petroleum news and statistics, abstracts, notices of new publications, and announcements of general pertinence to Oklahoma geology. Single copies, $1.50; yearly subscription, $6. Send subscription orders to the Survey at 100 E. Boyd, Room N-131, Norman, OK 73019. Short articles on aspects of Oklahoma geology are welcome from contributors; general guidelines will be sent on request.

This publication, printed by the Oklahoma Geological Survey, Norman, Oklahoma, is issued by the Oklahoma Geological Survey as authorized by Title 70, Oklahoma Statutes 1981, Section 3310, and Title 74, Oklahoma Statutes 1981, Sections 231–238. 1,500 copies have been prepared for distribution at a cost of $1,324 to the taxpayers of the State of Oklahoma. Copies have been deposited with the Publications Clearinghouse of the Oklahoma Department of Libraries.

OKLAHOMA GEOLOGY
Notes

CONTENTS

April 1998
VOL. 58, NO. 2

AVO Analysis of a Pennsylvanian Channel Sandstone in the Arkoma Basin, Oklahoma

Eric R. Kubera[1] *and Roger A. Young*[2]

Abstract

A seismic line that images a Pennsylvanian gas-producing channel sandstone in the Hartshorne Formation in the western Arkoma basin was acquired in September 1994. The data set was processed to retain true relative seismic reflection amplitudes and then analyzed for anomalous amplitude behavior. The results were displayed as attribute stack plots, which were examined for information that would describe the nature of the amplitude anomalies.

The reflection event interpreted as the top of the productive channel stands out on the seismic section and shows significant amplitude variation. The AVO (amplitude variation with offset) signature of the channel sandstone is characterized as that of a positive normal incidence reflection of moderate relative amplitude that displays a strong increase in amplitude with increasing offset.

Introduction

In September 1994, a seismic reflection line was presented to the School of Geology and Geophysics, University of Oklahoma, by the Pathfinder Group, LLC, Norman, for student use in master's degree research. This seismic line was acquired along a section road in T. 4 N., R. 12 E., Pittsburg County, Oklahoma (Fig. 1). It crosses the Hartshorne sandstone, a Pennsylvanian (Desmoinesian) gas-producing unit constituting the Ashland Field in this area, for which the Conoco No. 1-28 Lane was the discovery well.

Preliminary processing and amplitude display indicated that the portion of the stacked seismic line directly over the Hartshorne channel was high amplitude compared with the amplitude on either side of the channel. This was of interest because a classic study of the Hartshorne (Rutherford and Williams, 1989) suggested that a high-impedance gas sand, such as the Hartshorne, would give a dim out (decrease in amplitude) on a stacked section. The apparent difference in expected and actual response in initial processing prompted the AVO analysis described in this paper.

Production History of the Hartshorne

The Hartshorne sands produce natural gas in a trend that extends more than 70 mi across Haskell, Hughes, and Pittsburg Counties (Jason Hamilton, personal communication, 1995–96). Structure is the main trapping mechanism; the dominant drive mechanism is pressure depletion; and recovery is estimated to be 80% (Brown and Parham, 1994).

---

[1] Geophysicist, BHP Petroleum (Americas), Houston, Texas.
[2] School of Geology and Geophysics, University of Oklahoma.

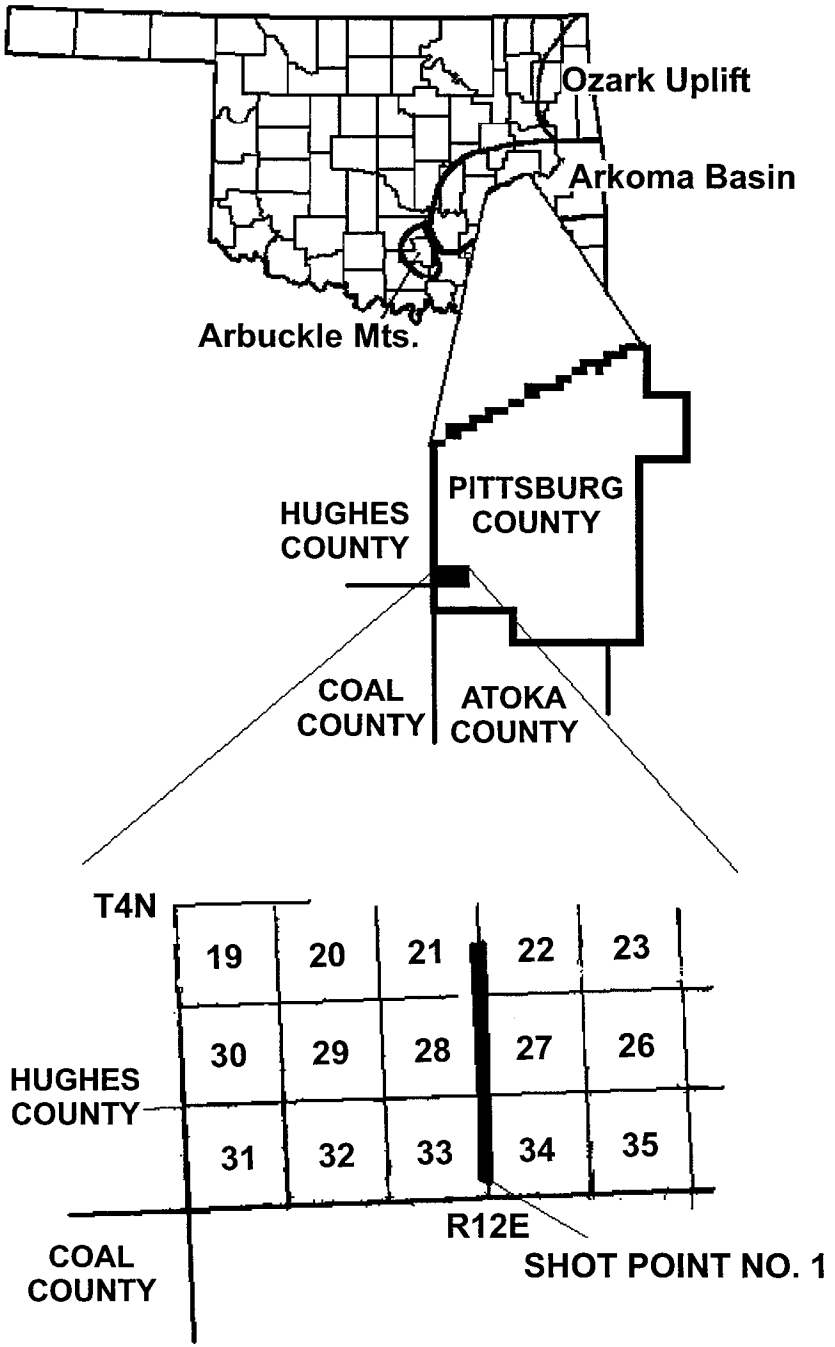

Figure 1. Map showing the study area and the location of the seismic line.

Depositional System of the Hartshorne

The Hartshorne Formation was deposited during the Desmoinesian (Middle Pennsylvanian) in a tidally influenced delta system that prograded from east to west into the Arkoma basin (Houseknecht and others, 1983). In the northern portion of the basin, the Hartshorne consists of a single sandstone unit and a single overlying coal unit (Friedman, 1982). In the area of this study, however, the coal unit is missing. Differential compaction of the sediments in the area made the thick channel a topographic high, and the coal-forming marsh areas collected on the flanks of the channel (J. M. Forgotson, personal communication, 1994–96). Based on logs in the area, the isolated Hartshorne channel in this study has been interpreted to be ~1 mi wide and 220–230 ft thick (Jason Hamilton, personal communication, 1995–96).

Seismic Data Acquistion

The seismic data were recorded by a Bison 9120A seismograph with 96 live channels deployed in a stationary array. Receiver spacing was 110 ft and shot spacing, 55 ft. The survey totaled 191 shots. Twelve Oyo Geospace model 20D-10 Hz geophones formed an array 110 ft in length. Field recording filters were 8 Hz low cut and 250 Hz high cut. The maximum offset used in CMP gather amplitude analysis was 6,200 ft.

The surface point source was a Bison Elastic Wave Generator III (EWG). Energy is released by the EWG when a vertically mounted iron beam is forced down onto a strike plate on the ground.

AVO Analysis in Brief

AVO (amplitude variation with offset, or amplitude versus offset) analysis is the investigation of seismic compressional-wave (P-wave) reflection data in search of a characteristic change in the amplitude of a reflection event with an increase in source-receiver offset and associated angle of incidence. The reflection of a plane wave from a boundary between two layers of differing elastic properties is well known (Zoeppritz, 1919). After appropriate processing, one can assume that the relative amplitude of the wave as recorded at different surface locations is proportional to the relative change in reflection coefficient associated with each reflection raypath connecting a source to a receiver by means of a common reflection point.

The reflection coefficient is dependent upon the angle of incidence of a seismic ray. The pattern of amplitude variation with offset can be determined by gathering together those traces representing reflections from a common reflection point (or common depth point [CDP]) (Fig. 2). This pattern of amplitude variation with offset is called the AVO response of a target boundary. Because the elastic properties of the earth will vary along a boundary, so also will the AVO response.

The key factor that makes AVO analysis useful is that, at a shale-sandstone boundary, the presence of gas in a sandstone plays a major role in determining the reflection response of a compressional wave. However, amplitude variation with offset may be due also to propagation effects unrelated to variations in the reflection coefficient, and the amplitude information about the presence or absence of gas may be completely overwhelmed by these non-hydrocarbon effects. Amplitude compensation, to remove non-hydrocarbon effects, is called true relative amplitude processing. It requires different strategies than does processing for geologic structure, in which determination of amplitude variation with offset is not a goal.

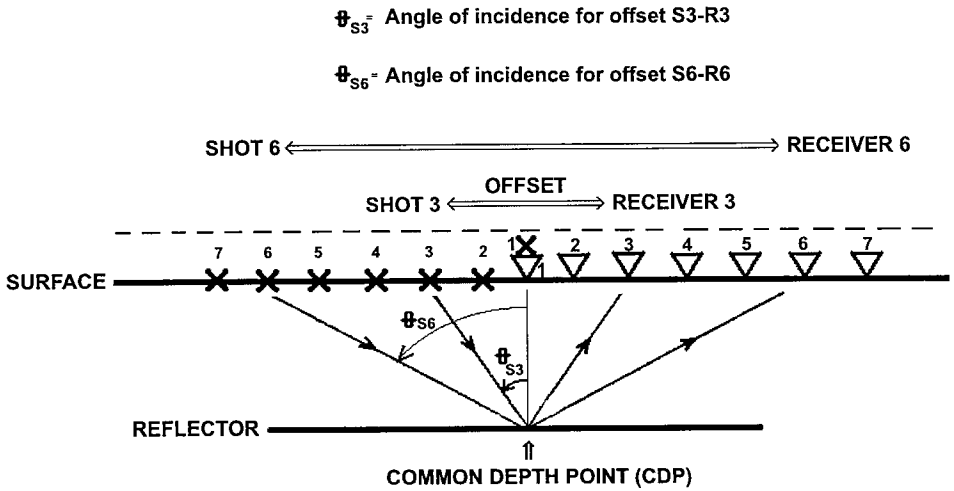

Figure 2. Schematic representation of the relationship between shot-receiver distance (called offset) and the associated angle of incidence (θ) at the reflector. Note that an increase in offset results in an increase in the angle of incidence.

How AVO Analysis is Performed

If one removes all amplitude variation that could be attributed to causes other than the presence of hydrocarbon, an AVO pattern may remain. It may be due to the presence of gas, or it may be due to lithologic variation (including the presence of non-hydrocarbon fluids, such as brine). In an ideal situation, the background trend in AVO response due to non-hydrocarbon-bearing rocks is established, and one searches for deviations from this norm, as these deviations may be the "fingerprints" of hydrocarbon.

After true relative amplitude processing, one commonly examines CMP gathers for an AVO pattern. In the present case, however, the data were so noisy that even after processing it was not possible to see an amplitude variation on the CMP gathers themselves. For this reason, an automated procedure that characterizes the amplitude pattern by two quantities, an intercept and a gradient, was adopted in this study. This procedure is called AVO attribute analysis. It produces attribute stacks and, in so doing, smooths the data.

Relative Amplitude Processing

Our processing sequence (Fig. 3) followed conventional methods (Allen and Peddy, 1993, p. 22, fig. 25) for the most part and included elevation statics correction; spherical divergence correction; receiver array compensation; shot and receiver balancing; semblance and constant velocity analysis and normal moveout correction; residual statics correction; supergather formation; deconvolution; bandpass filtering; trace equalization; and the calculation of angle gathers (Kubera, 1996). In order to determine optimal parameters for each step in the processing scheme, initial parameter testing was conducted. Automatic gain control (AGC) was used in velocity analysis, deconvolution, and filtering tests. AGC distorts rela-

tive amplitudes, however, and was not applied during actual processing. Because the data were very noisy due to cultural disturbances, bandpass filtering was done at an early stage, as well as after deconvolution. No ramp gain was applied after spherical divergence correction. An important additional step of trace equalization was used. Tests on synthetics showed that applying trace envelope gain destroyed the amplitude versus offset pattern (Kubera, 1996). In contrast, trace equalization by a constant value, determined by the RMS (root mean square) amplitude in a time window, did not change the pattern. The window was carefully chosen to include events that did not display an AVO effect (Kubera, 1996).

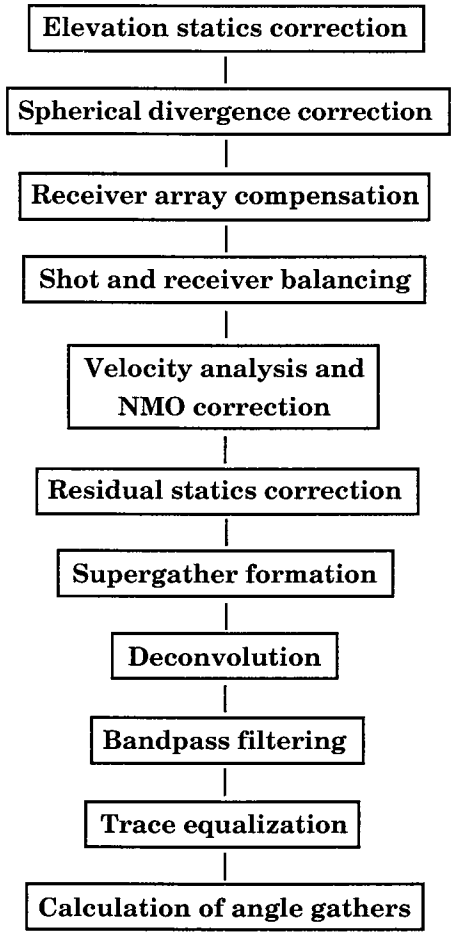

Figure 3. The true relative amplitude processing sequence used in this study.

Identifying the Hartshorne Event on the Processed Seismic Section

The sonic and density logs for the Conoco No. 1-28 Lane well (sec. 28, T. 4 N., R. 12 E.) were digitized. The interpreted depth to the top of the Hartshorne was taken from the scout ticket for the No. 1-28 Lane well to mark the formation top. The log and formation top were imported into well editing software and used to create a synthetic seismogram. Figure 4 shows the velocity log, formation top, and synthetic. The wavelet used in the synthetic was extracted statistically from a portion of seismic trace by minor editing of the amplitude spectrum from 300 ms to 700 ms (Kubera, 1996, p. 81). This window contains several repetitions of the wavelet from primary reflections.

The synthetic seismogram, in normal and reverse polarity (Fig. 4), was compared with an AGC version of the seismic section in order to determine the timing of the Hartshorne reflection (Fig. 5). Correlation between the stacked section and the synthetic shows that the reflection from the channel top is located at 680 ms, beneath shot number 209 on Figure 5. The extent of the channel is interpreted to be from CMP number 331 to CMP number 481 on Figure 6.

Calculation of AVO Attribute Stacks

After processing is completed, AVO attribute stacks are calculated. Events have been NMO (normal moveout) corrected at this stage and can be distinguished au-

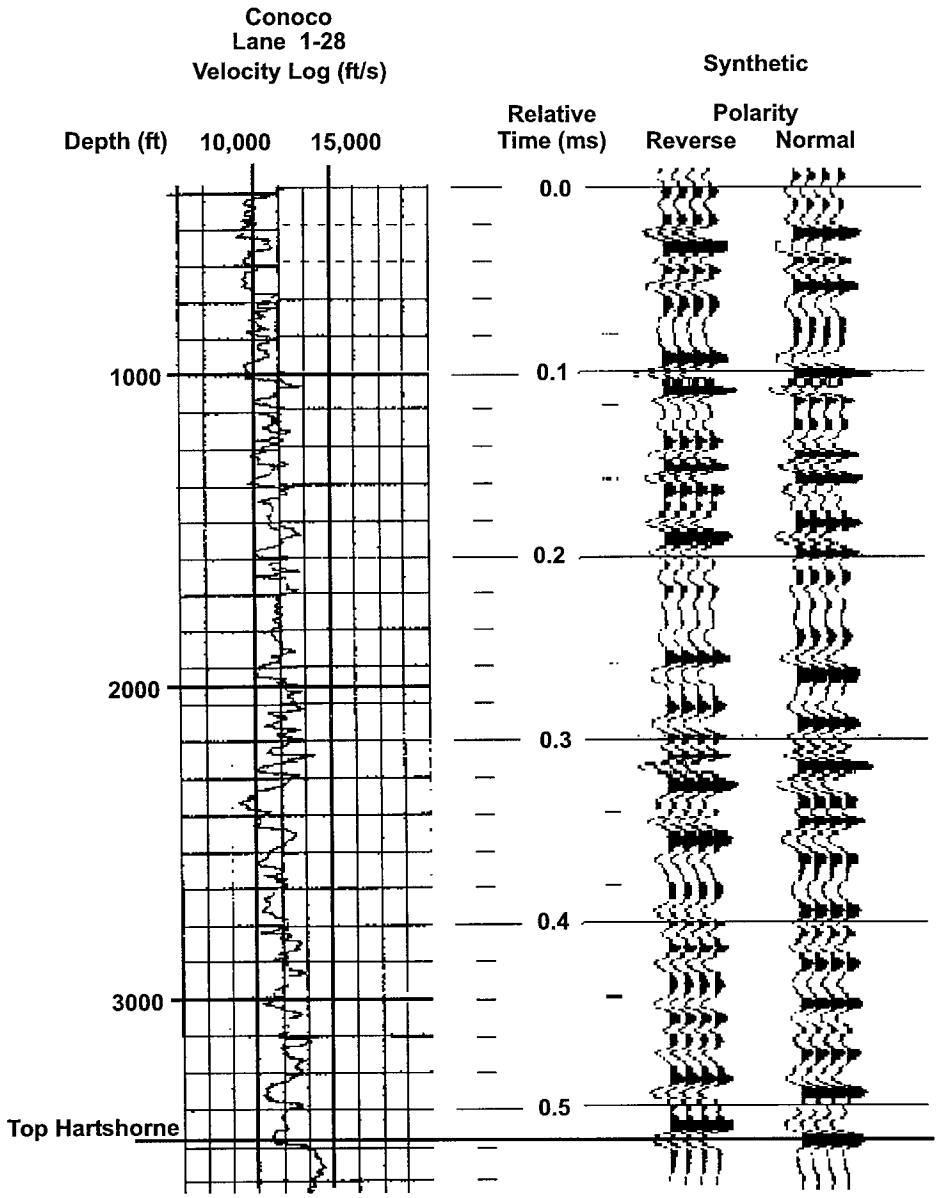

Figure 4. The velocity log corresponding to the sonic log from the Conoco No. 1-28 Lane well and the synthetic seismogram (generated from the velocity and density logs).

tomatically by the polarity gate within which each event falls. Figure 7 shows a pilot trace formed by summing individual traces. Two consecutive zero crossings of the stacked trace are extended horizontally to form bounds that bracket the event. This is the polarity gate. Extremely short intervals bracketing noisy events do not qualify

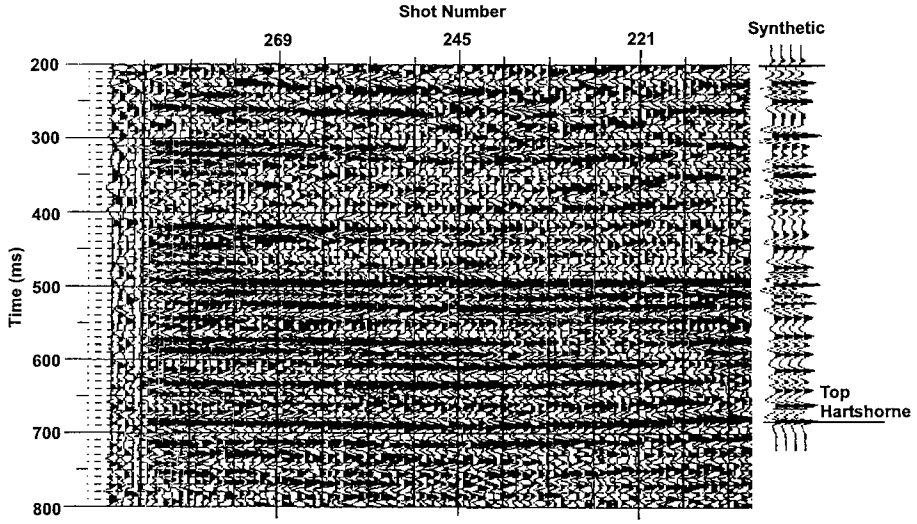

Figure 5. Diagram showing the correlation of the synthetic seismogram (right) with the stacked section (left). The reflection peak at 680 ms is identified as the reflection from the top of the Hartshorne. The synthetic ends at 720 ms because the sonic log ends at the corresponding depth.

as a polarity gate. The maximum amplitude within the gate is calculated for each offset. Offset is converted to angle of incidence, θ, using rays in a one-dimensional model formed from an interval velocity function provided by the user. A plot of relative amplitude versus $\sin^2\theta$ is made. This plot of amplitudes is linear (Shuey, 1985), given that relative amplitudes are proportional to reflection coefficients, and a least-squares fit of the values for each trace is performed (Fig. 8). From this plot come the two characteristics of the line: its slope, or gradient, and its intercept. The gradient is positive if amplitudes increase with angle of incidence (or, equivalently, with offset). The intercept is the amplitude when $\theta = 0$, that is, at normal incidence. This intercept value is the relative normal incidence reflection coefficient because, after processing, amplitudes are proportional to reflection coefficients.

The two values, intercept and gradient, are called AVO attributes. They characterize a particular reflection event and are calculated for each CMP. Intercept and gradient are, therefore, calculated in time for each polarity gate and in position at each CMP location. It is possible, then, to make a two-dimensional plot of either attribute, using color to represent the value of the attribute. The color represents one of the following: the magnitude (the absolute value of the attribute), its sign (negative or positive), or the signed magnitude. Because each CMP location has an attribute value at each time, as in a CMP stacked section, such a plot is called an attribute stack. The two basic attributes, intercept and gradient, can be combined as a sum or product, for example, to give new attributes.

Interpretation of Attribute Stack Plots

During relative amplitude processing, amplitudes are normalized by the average amplitude of a reference event. This means that attribute stacks also show relative

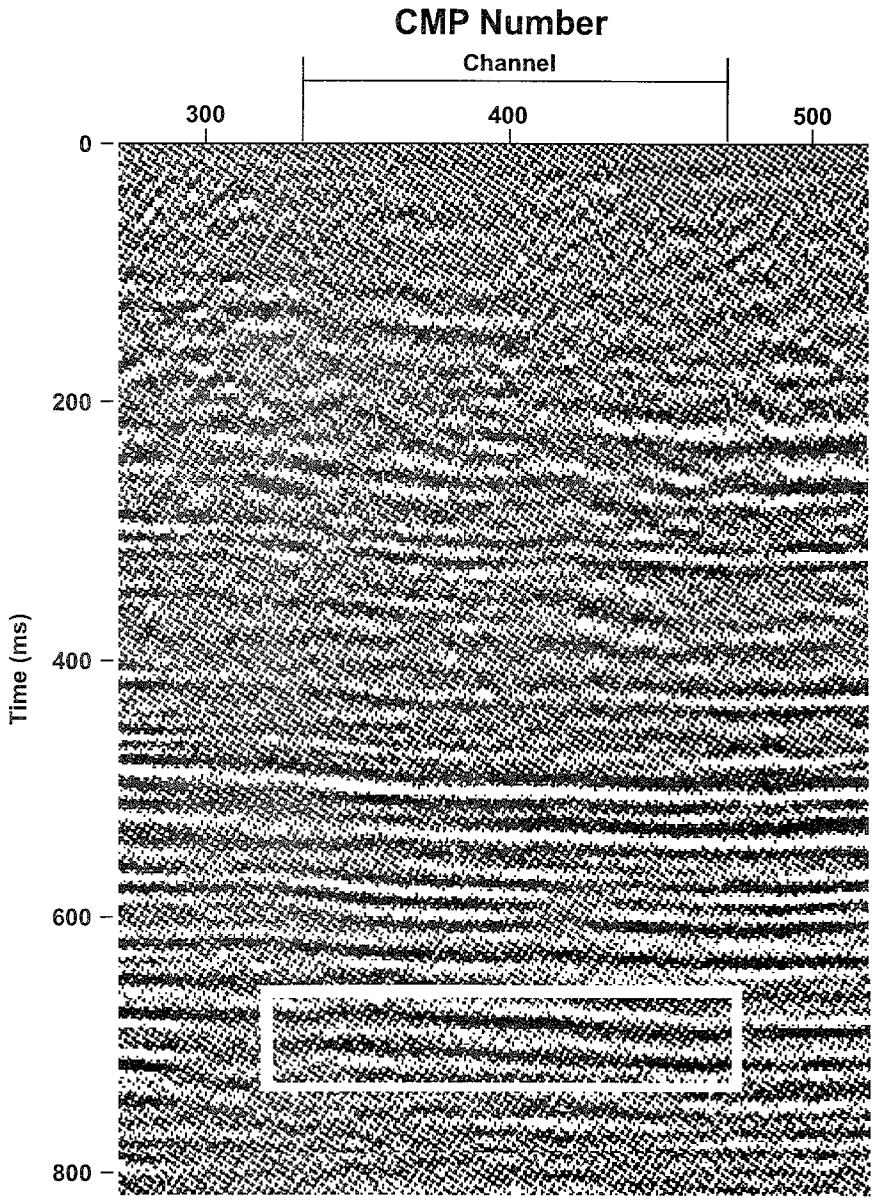

Figure 6. AGC stacked section showing the interpreted extent of the Hartshorne channel in the study area.

variation, not absolute values. In addition, further scaling was performed by the ProMAX modules (Advance Geophysical Corporation, 1995) used to generate the attribute stack plots (Figs. 9–12).

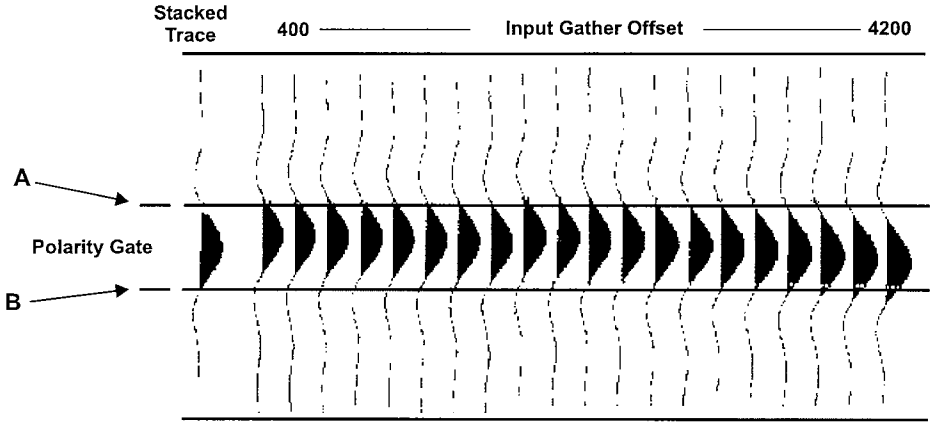

Figure 7. Diagram showing how a stacked pilot trace is used to determine the time limits of a polarity gate. A pilot trace is formed by stacking traces in a CMP gather. Lines at two consecutive zero crossings of the stacked trace (A and B) are extended across the CMP gather to determine a polarity gate by bracketing the event. For each offset, the maximum amplitude within this gate is calculated.

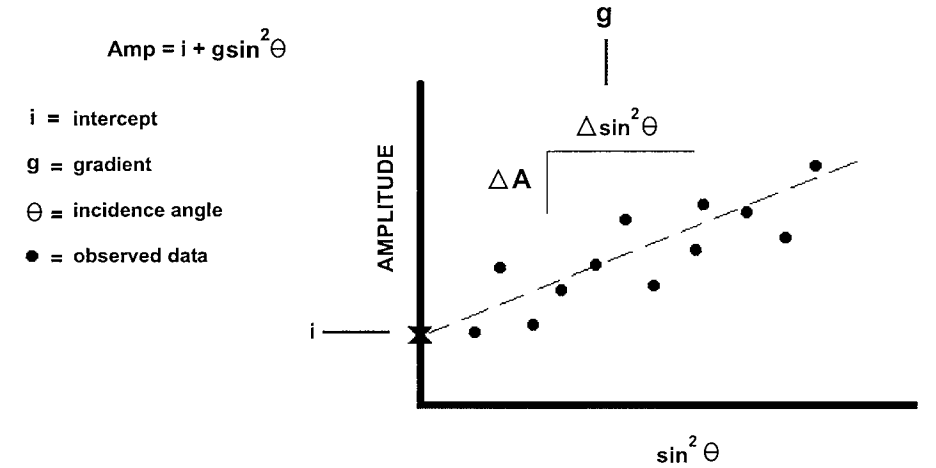

Figure 8. Amplitudes of an event, taken from its polarity gate (see Fig. 7) and plotted (dots) against $\sin^2\theta$, where θ is the angle of incidence for the event. The best-fit line (dashes) has an intercept (i) and a gradient (g) that characterize the amplitude behavior of this particular event. A new plot is formed for each polarity gate and for each CMP location. These plots can then be combined into a two-dimensional plot, either of intercept or gradient, which is called an attribute stack.

The first attribute is the intercept (Attribute No. 1, ProMAX Reference Manual [Advance Geophysical Corporation, 1995]). Figure 9 (bottom) shows the color scale for the intercept attribute. Red to white colors (hot colors) correspond to positive normal incidence reflection coefficients, and white to gray colors (cold colors) cor-

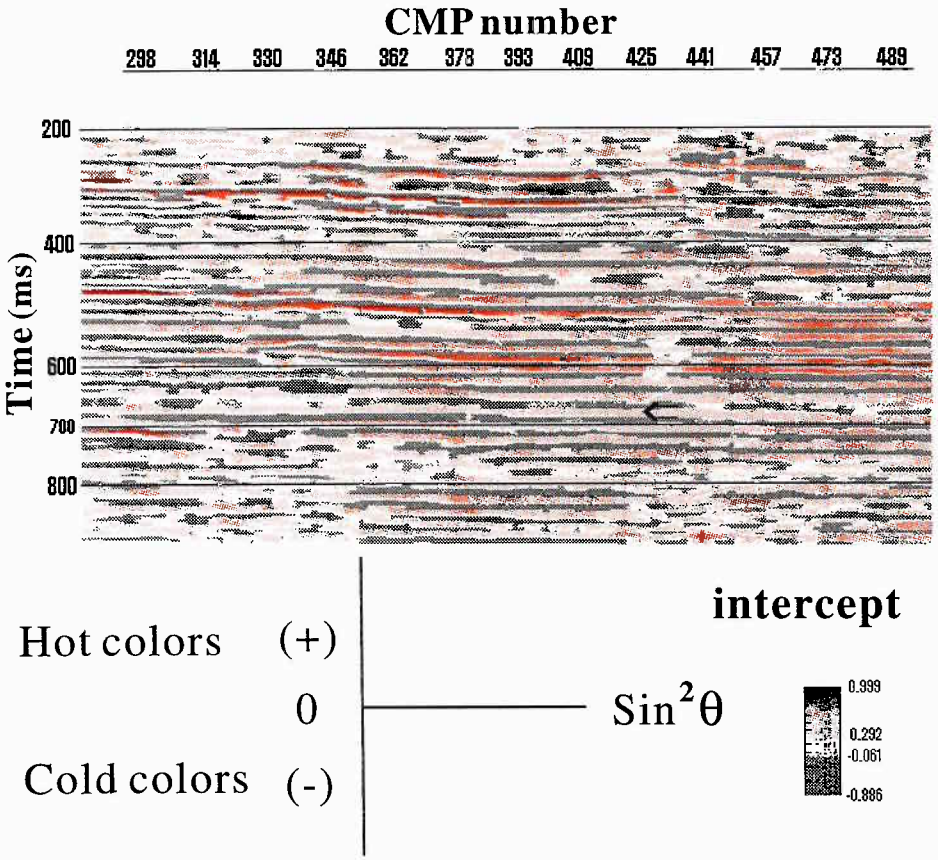

Figure 9. Stack plot of the intercept attribute. Note the bright reflectors at 300 ms, 500 ms, and 600 ms. The Hartshorne reflection (arrow) occurs at ~680 ms, under CMP number 419, and is relatively faint. Positive intercept values are shown as hot colors (red to white); negative intercept values are shown as cold colors (white to gray).

respond to negative normal incidence coefficients. The intercept plot for the data set is shown in Figure 9 (top). Noticeable reflectors at 300 ms, 500 ms, and 600 ms on this plot correspond to strong reflection events on the stacked section (Fig. 5). No geologic correlation has been made to identify the formations associated with these high amplitude, normal incidence reflections.

An earlier AVO study of the Hartshorne sandstone suggests that the channel should be a high-impedance boundary that would produce a positive intercept on the AVO plot (Rutherford and Williams, 1989). The velocity log (Fig. 4) shows the interpreted top of the channel to have a significantly large increase in P-wave velocity. However, the intercept attribute stack plot (Fig. 9) does not show a significantly large intercept value for the Hartshorne reflection (arrow at 680 ms). This plot is useful, but it is not sufficient in itself to characterize the amplitude behavior of the Hartshorne reflection event.

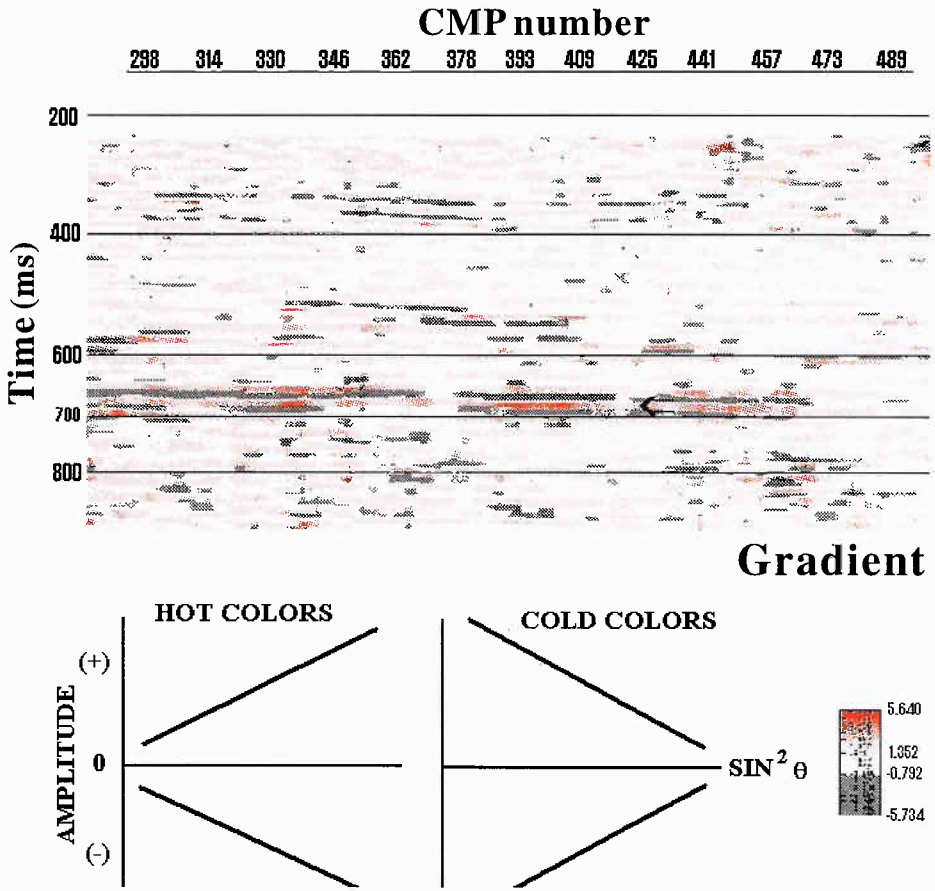

Figure 10. Stack plot of the Gradient attribute. The Gradient is positive (hot color: red to white) if a peak grows to a larger peak with increasing offset or if a trough grows to a larger trough with increasing offset. Otherwise, it is negative (cold colors: white to gray). Note the significant Gradient values in the time zone of interest (660–700 ms). These are large relative to other parts of the section.

The second attribute is the Gradient (Attribute No. 2, ProMAX Reference Manual [Advance Geophysical Corporation, 1995]). On the AVO plot (Fig. 8), the gradient is the slope of the best-fit line, and it describes the relative change in reflection amplitude with change in incidence angle. A related attribute, the ProMAX Gradient attribute, is shown in Figure 10 (top). This Gradient attribute is positive (hot colors) if a peak grows to a larger peak with increasing offset or a trough grows to a larger trough with increasing offset (Fig. 10, bottom). If the amplitude decreases, the value is negative (cold colors).

In the interval of interest (660–700 ms) on the Gradient attribute stack plot (Fig. 10), there are three features that show pronounced Gradient characteristics. A relatively continuous event at ~670 ms (arrow) shows a strong Gradient in gray be-

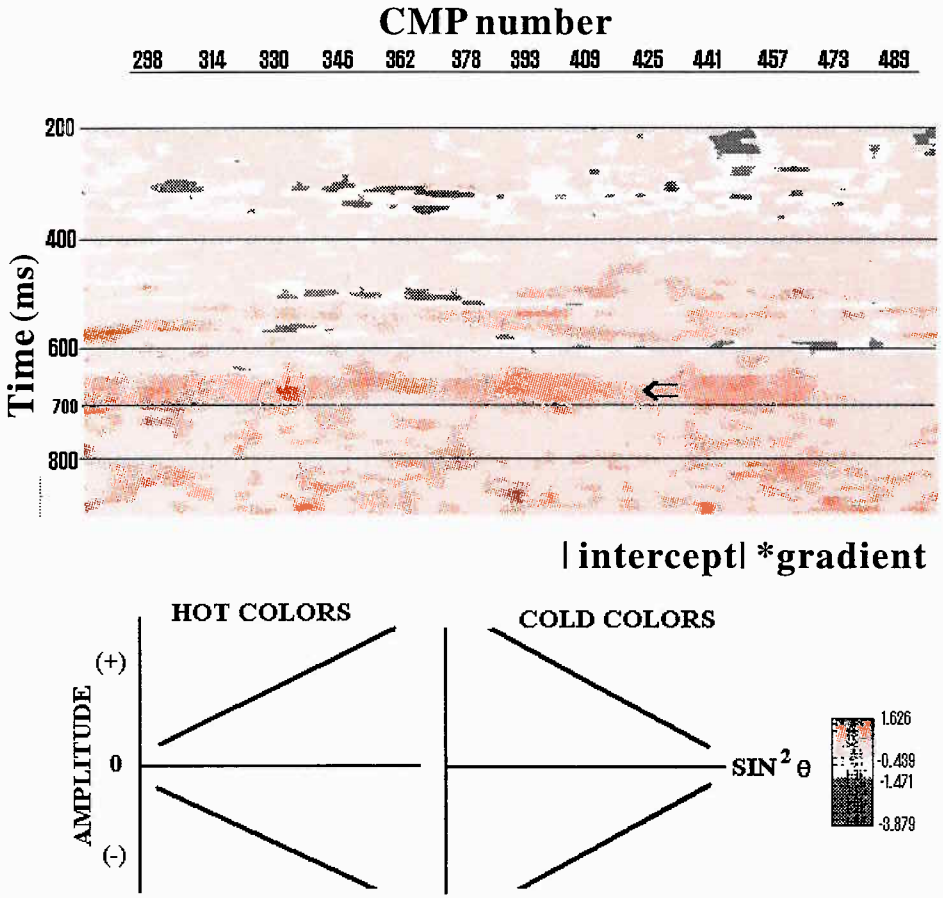

Figure 11. Stack plot of the |intercept|*gradient attribute. Large values are shown in the zone of interest, 660–700 ms.

tween CMP numbers 282 and 457. That event is followed by a discontinuous event in red, at ~680 ms, under CMP numbers 330, 393, and 441. And, finally, a third event in gray, at ~690 ms, shows strong, discontinuous Gradient characteristics between CDP numbers 282 and 457 (coinciding slightly with the strong Gradient portions of the event above it). On the stack shown in Figure 5, the Hartshorne reflection event is preceded and followed by relatively strong troughs. The strong Gradient event shown in red on Figure 10, therefore, is interpreted to be the Hartshorne reflection. It is obvious that the zone of interest contains the strongest Gradient values in the plot and that these values are positive. Although, by itself, this plot does not describe the AVO effect completely, it does provide evidence of increase in amplitude with offset in the zone of interest.

The third attribute is the |intercept|*gradient (Attribute No. 3, ProMAX Reference Manual [Advance Geophysical Corporation, 1995]). This attribute is the product of the intercept's absolute value and the gradient. It highlights reflection events

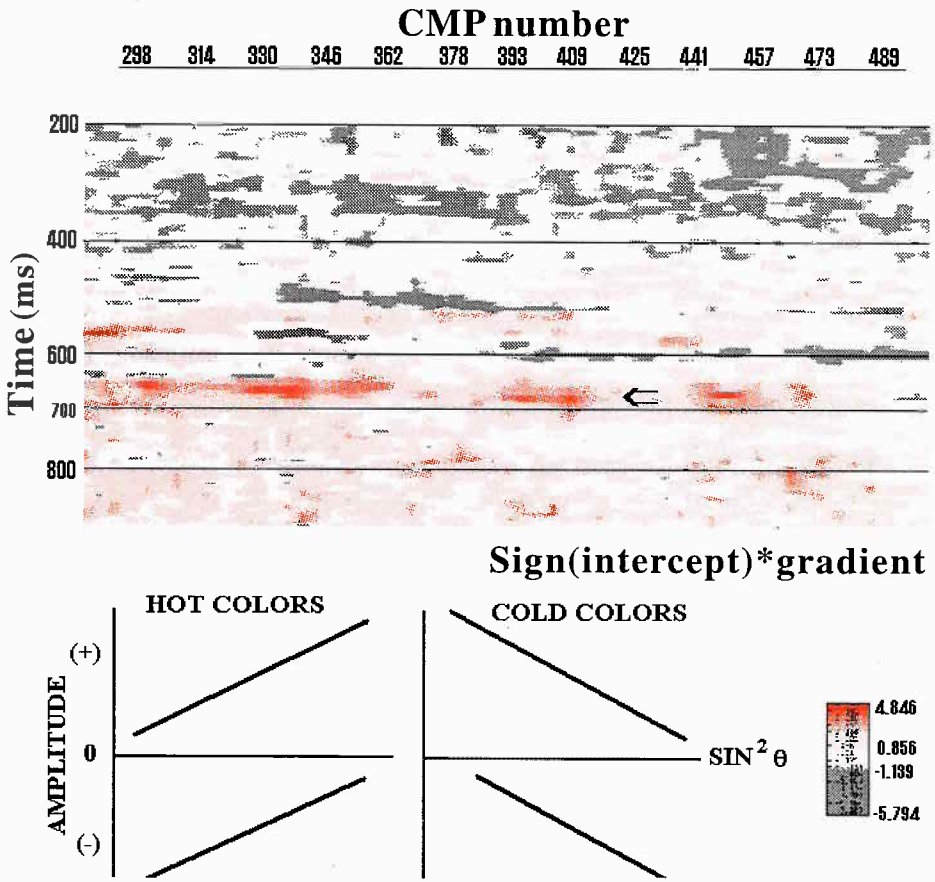

Figure 12. Stack plot of the Sign (intercept)*gradient attribute. This plot is different from the one in Figure 11 in that this attribute depends upon the signs of both the intercept and the gradient. Large values appear at ~680 ms.

that show both a strong normal incidence reflection coefficient and a large AVO effect. The sign of the attribute is determined by the sign of the gradient. The |intercept|*gradient plot of the Hartshorne data is shown in Figure 11 (top). On the plot, an increase in this attribute is a hot color (red to white) and a decrease in value is a cold color (white to gray) (Fig. 11, bottom). Note that the AVO patterns of Figure 11 (bottom) and Figure 10 (bottom) are the same.

The |intercept|*gradient attribute stack plot (Fig. 11) is divided into two areas. Data above 600 ms are dominated by negative values (cold colors), which indicate a decrease in relative amplitude. Data below 600 ms are dominated by positive values (hot colors), which indicate an increase in relative amplitude. The strong, discontinuous areas above and below the zone of interest are interpreted to be places where the low signal-to-noise ratio allowed non-signal amplitude values to show a trend in the gradient. The zone of interest (660–700 ms; CMP numbers 282–473)

stands out against the rest of the data because of the continuous pattern of high values. Although the zone of interest does not have a strong presence in the intercept plot (Fig. 9), it does show strong character in the Gradient plot (Fig. 10). Therefore, when the intercept and gradient magnitudes are multiplied together, the zone of interest becomes more visible. Conversely, when the magnitudes for the strongest events on the intercept plot (at 300 ms, 500 ms, and 600 ms) are multiplied by the relatively weak gradient magnitudes, those events become less visible. The values of the |intercept|*gradient attribute associated with the zone of interest indicate that the AVO signature for the Hartshorne reflection is an increase in reflection amplitude with offset.

The product of the |intercept|*gradient attribute has the same sign as the gradient attribute, and Figures 10 and 11 are very similar. They both support the inference that the Hartshorne reflection increases in amplitude with offset. Analysis of the next attribute reveals whether this increase in amplitude is a peak increasing in size or a trough increasing in size.

The fourth, and final, attribute is the Sign(intercept)*gradient (Attribute No. 4, ProMAX Reference Manual [Advance Geophysical Corporation, 1995]). The magnitude of this attribute is the magnitude of the gradient, and the sign of the attribute takes the sign of the product of the signs of the gradient and the intercept.

The Sign(intercept)*gradient attribute stack plot for the Hartshorne data is shown in Figure 12 (top). The zone of interest (660–700 ms) shows a relatively clear, but discontinuous, event in red, a hot color. Because the |intercept|*gradient attribute showed that the gradient is positive, the intercept must also be positive. Recall that the synthetic seismogram (Fig. 5) established that the reflection is a peak (positive intercept). Both of these deductions are convincing evidence for a positive intercept.

The evidence from the synthetic seismogram and from the AVO attribute stack plots is consistent and supports a positive zero-offset reflection characterized by a peak that becomes stronger in amplitude with increasing offset.

Discussion of Results

The principal conclusion of the present work is that the reflection from the top of the Hartshorne Formation in the study area has a distinctive variation in amplitude with offset. This response is found to have a positive normal incidence reflection coefficient that increases in amplitude with increasing offset. A classic study by Rutherford and Williams (1989) found that, elsewhere, the reflection from a productive Hartshorne channel sandstone displayed a dim out (decrease in amplitude) on a stacked section. This dim out was inferred to be due to a decrease in amplitude with offset.

The difference between Rutherford and Williams (1989) and the present study has a simple explanation. Originally we had questioned whether our maximum offset was large enough to observe a dim out. The maximum offset we used in the AVO attribute stacks, however, is 6,200 ft, giving an offset-to-target-depth ratio of approximately two. Rather than being insufficiently large, this is so large, in fact, that our reflection angles are approaching critical. The Shuey (1985) approximation of a linear AVO response is valid only for angles of incidence of <30°. For traces dominated by much larger angles of reflection, the amplitude must increase with offset. This is the major reason for a difference between the two studies.

Other effects may also play a secondary role in the difference. We do not know the location of the Rutherford and Williams (1989) survey with respect to ours,

and one suspects that different locations within the Hartshorne would have different residual gas saturations. How different might the resultant AVO responses be? Even after production, residual gas saturation is likely to be 20%. Inasmuch as 5–10% gas saturation is all that is necessary to change Vp/Vs substantially (Allen and Peddy, 1993), production cannot, it seems, explain fully the differing AVO responses.

The present study occurs in an area where the coal seam overlying the Hartshorne is missing. This may account for the small normal incidence reflection coefficient we obtained. It is also likely that a major contribution to differing AVO responses is a difference in lithology leading to different background trends (see Castagna and Swan, 1997, p. 338). If the AVO analysis of the present CMP gathers and of the CMP gathers associated with the stacked section of Rutherford and Williams (1989) were each compared to an appropriate background trend established by crossplotting, then the differences between the two might not be so great as it appears to be in the unadjusted data.

Additional Study

The Elastic Wave Generator (EWG) source did not provide sufficient energy to allow us to examine amplitudes at large offsets on CMP gathers. We recommend the use of a larger EWG or of small dynamite charges. Acquisition design dictated that the geophones be planted in unconsolidated material in and near drainage ditches at the sides of the section roads followed by the seismic line. We also recommend that special care be used in planting geophones, perhaps farther from the unconsolidated material in drainage ditches.

Sonic logs are available from throughout the Hartshorne (Larry Lunardi, personal communication, 1998). AVO modeling at many wells would provide information on trends in AVO response due to lithological variation for different regions of the Hartshorne. Then, in future exploration in the Hartshorne, adjusting data for such background trends could help isolate seismic signals indicative of hydrocarbon-bearing channel sands.

Summary

Using the well logs from the Conoco No. 1-28 Lane well and the four attribute stack plots created by an amplitude-sensitive processing scheme, the top of the Hartshorne Formation in the study area was positively identified as a reflection from a known gas-bearing channel sandstone. The distinctive AVO response of this interval is characterized as that of a positive normal incidence reflection of moderate amplitude that increases in amplitude with increasing offset. It differs from the earlier result of Rutherford and Williams (1989), but a comparison may be inappropriate because the maximum offsets used in the two studies are very different and the lithologies at the two sites may not be the same. The AVO signature identified in the present study could be helpful in tracking the target horizon on stacked sections acquired in the immediate area.

Acknowledgments

We would like to thank the Pathfinder Group, LLC, Norman, for allowing us to use their Ashland Field data set. We are grateful to Larry Lunardi and John Castagna for discussions that led to the improvement of this paper.

References Cited

Advance Geophysical Corporation, 1995, ProMAX operating manual, version 6.0, v. 1: Advance Geophysical Corporation, Denver, 860 p.

Allen, J. L.; and Peddy, C. P., 1993, Amplitude variation with offset: Gulf Coast case studies: Society of Exploration Geophysicists, Tulsa, 126 p.

Brown, R. L.; and Parham, K. D., 1994, Desmoinesian fluvial and deltaic sandstone, Arkoma basin, Oklahoma and Kansas, *in* Bebout, D. G.; White, W. A.; Hentz, T. F.; and Grasmick, M. K. (eds.), Atlas of major Midcontinent gas reservoirs: Gas Research Institute, Bureau of Economic Geology, Austin, Texas, p. 36–39.

Castagna, J. P.; and Swan, H. W., 1997, Interpreter's corner—principles of AVO crossplotting: The Leading Edge, v. 16, p. 337–344.

Friedman, S. A., 1982, Determination of reserves of methane from coal beds for use in rural communities in eastern Oklahoma: Oklahoma Geological Survey Special Publication 82-3, 32 p.

Houseknecht, D. W.; Zaengle, J. F.; Steyaert, D. J.; Matteo, P. A., Jr.; and Kuhn, M. A., 1983, Facies and depositional environments of the Desmoinesian Hartshorne sandstone, Arkoma basin, *in* Houseknecht, D. W. (ed.), Tectonic-sedimentary evolution of the Arkoma basin: Society of Economic Paleontologists and Mineralogists, Midcontinent Section, v. 1, p. 53–82.

Kubera, Eric, 1996, Relative amplitude processing: an AVO investigation of a Pennsylvanian age channel sandstone in the Arkoma basin, Oklahoma: University of Oklahoma unpublished M.S. thesis, 117 p.

Rutherford, S. R.; and Williams, R. H., 1989, Amplitude-versus-offset variations in gas sands: Geophysics, v. 54, p. 680–688.

Shuey, R. T., 1985, A simplification of the Zoeppritz equations: Geophysics, v. 50, p. 609–614.

Zoeppritz, K., 1919, Erdbebenwellen VIII B, On the reflection and penetration of seismic waves through unstable layers: Gottinger Nachr, v. 1, p. 66–84.

OKLAHOMA EARTHQUAKES, 1997

James E. Lawson, Jr.,[1] *and Kenneth V. Luza*[2]

Introduction

More than 930,000 earthquakes occur throughout the world each year (Tarbuck and Lutgens, 1990). Approximately 95% of these earthquakes have a magnitude of <2.5 and are usually not felt by humans (Table 1). Only 20 earthquakes, on average, exceed a magnitude 7.0 each year. An earthquake that exceeds a magnitude 7.0 is considered to be a major earthquake and serious damage could result.

Earthquakes tend to occur in belts or zones. For example, narrow belts of earthquake epicenters coincide with oceanic ridges where plates separate, such as in the mid-Atlantic and east Pacific Oceans. Earthquakes also occur where plates collide and/or slide past each other. Although most earthquakes originate at plate boundaries, a small percentage occur within plates. The New Madrid earthquakes of 1811–12 are examples of large and destructive intraplate earthquakes in the United States.

The New Madrid earthquakes of 1811 and 1812 are probably the earliest historical earthquake tremors felt in Oklahoma (Arkansas Territory) by residents in southeastern Oklahoma settlements. Before Oklahoma became a state, the earliest

TABLE 1. — ESTIMATED NUMBER OF WORLDWIDE EARTHQUAKES PER YEAR BY MAGNITUDE
(Modified from Tarbuck and Lutgens, 1990)

Magnitude	Estimated number per year	Earthquake effects
<2.5	>900,000	Generally not felt, but recorded
2.5–5.4	30,000	*Minor to moderate earthquakes* Often felt, but only minor damage detected
5.5–6.0	500	*Moderate earthquakes* Slight damage to structures
6.1–6.9	100	*Moderate to major earthquakes* Can be destructive in populous regions
7.0–7.9	20	*Major earthquakes* Inflict serious damage if in populous regions
≥8.0	1–2	*Great earthquakes* Produce total destruction to nearby communities

[1]Oklahoma Geological Survey Observatory, Leonard.
[2]Oklahoma Geological Survey.

documented earthquake occurred October 22, 1882, probably near Fort Gibson, Indian Territory, although it cannot be located precisely (Ross, 1882; Indian Pioneer Papers, date unknown). The *Cherokee Advocate* newspaper reported that at Fort Gibson "the trembling and vibrating were so severe as to cause doors and window shutters to open and shut, hogs in pens to fall and squeal, poultry to run and hide, the tops of weeds to dip, [and] cattle to lowe" (Ross, 1882, p. 1). These observations indicate MM-VIII intensity effects. The next documented earthquake in Oklahoma occurred near Jefferson, Grant County, on December 2, 1897 (Stover and others, 1981). The next known Oklahoma earthquake happened near Cushing, Payne County, in December 1900. This event was followed by two additional earthquakes in the same area in April 1901 (Wells, 1975).

The largest known Oklahoma earthquake (with the possible exception of the 1882 earthquake) occurred near El Reno, Canadian County, on April 9, 1952. This magnitude-5.5 (mb, Gutenberg-Richter) earthquake was felt in Austin, Texas, as well as Des Moines, Iowa, and covered a felt area of ~362,000 km^2 (Docekal, 1970; Kalb, 1964; von Hake, 1976). From 1897 through 1997, 1,489 earthquakes have been located in Oklahoma.

Instrumentation

A statewide network of 11 seismograph stations was used to locate 117 earthquakes in Oklahoma for 1997 (Fig. 1). The Oklahoma Geological Survey Observatory station, TUL, located near Leonard, Oklahoma, in southern Tulsa County, records 15 continuous seismic signals from sensors located at four stations. The data are recorded, analyzed, and archived on a GSE digital seismic system provided by the Defense Advanced Research Projects Agency/Nuclear Monitoring Research Office.

Signals are digitized by one Geotech RDAS (Remote Data Acquisition System) unit at either 3,600 or 1,200 24-bit samples per second. The RDAS then applies digital anti-alias filtering to eliminate frequencies too high for the final sampling rate. After one to three digital filter and resampling stages, the RDAS produces 60, 40, 20, or 10 24-bit samples per second. The samples are time-tagged by RDAS clocks locked to low-frequency time signals from National Institute of Standards and Technology station WWVB. The signals are passed by RS422 serial links to an AST 386/25 RTDS (Real Time Data Server) computer, which has a Lynx™ real-time Unix-like operating system. The partially processed signals are passed by ethernet to a Sun Sparc 2+ Unix workstation with 64 megabytes of memory, two 660-megabyte disks, two 2.1-gigabyte disks, and two 2.5 gigabyte Exabyte™ tape drives. All of the data from the most recent two weeks are retained on disk. Each day, data from the preceding day (167 million bytes) are automatically archived onto Exabyte™ tape. All Oklahoma earthquakes, and other selected events, are placed in named de-archive directories on disk. An Oracle™ data base on the Sun Sparc 2+ keeps track of every second of data on the permanent archive tapes, the last 14 days' data on disk, and data in the de-archive directories. Data analysis is done by Teledyne-Geotech and Science Applications International Corp. software on the Sparc 2+ workstation.

The digital system signals are from three sensors in the Observatory vault (international station abbreviation TUL); from a three-component broadband sensor in a 120-m borehole; and from single sensors located at Rose Lookout (RLO) in Mayes County, at the Bald Hill Ranch near Vivian (VVO) in McIntosh County, and at the Jackson Ranch near Slick (SIO) in Creek County.

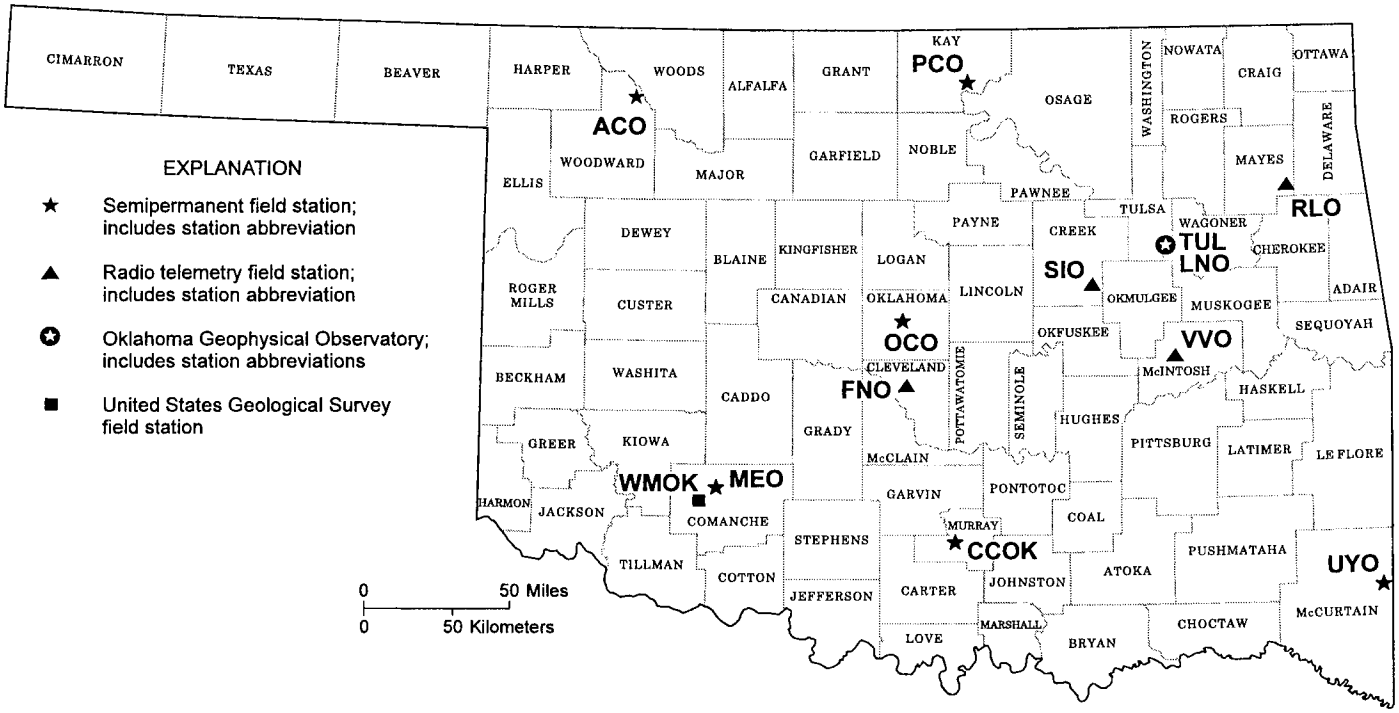

Figure 1. Active seismographs in Oklahoma.

TUL has three (vertical, north–south, east–west) Geotech GS-13 seismometers which produce 40-sample-per-second short-period signals. A three-component broadband Geotech KS54000-0103 seismometer in a 120-m-deep borehole produces seven digital data channels. Three are broadband signals from seismic signals in vertical, north–south, and east–west directions. From the broadband signals the Sparc 2+ workstation derives three long-period signals. A seventh signal, the vertical earth tides, is recorded from the vertical mass displacement signal from the KS54000-0103. The broadband signals are archived at 10 samples per second, and the long-period and vertical-earth-tide signals are recorded at one sample per second. On November 10, 1994, the broadband sample rate was increased from 10 samples per second to 20 samples per second. This increase was for two purposes. One was to allow the broadband bore-hole seismometer to record higher frequencies characteristic of Oklahoma earthquakes. The other was to make the signals compatible for the GSETT-3 (Group of Scientific Experts Technical Test-3), which began in 1995. GSETT-3 is a prototype international seismic-monitoring system to detect underground nuclear tests. Data segments will be copied automatically and sent to the International Data Center by Internet without affecting the recording and analysis of Oklahoma earthquakes.

RLO, VVO, and SIO have Geotech S-13 seismometers in shallow tank vaults. The seismic signals are amplified and used to frequency modulate an audio tone that is transmitted to Leonard with 500-mW FM transmitters at various frequencies in the 216–220-mHz band. The signals are received by antennas on a 40-m-high tower at Leonard, the tones are discriminated to produce a voltage which is proportional to the remote seismometer voltage, and the voltages are digitized at 40 samples per second by the vault RDAS.

A fourth radio-telemetry station, FNO, was installed in central Oklahoma on April 28, 1992. The seismometer, Geotech S-13, is located on a concrete pad, ~7 km northeast of the Oklahoma Geological Survey's (OGS) building. A discriminator converts the audio-signal frequency fluctuations to a voltage output. The voltage-output is amplified and recorded by a Sprengnether MEQ-800 seismograph recorder (located in an OGS display case) at 60 mm/min trace speed.

In the Leonard vault, seven additional seismometers produce analog (wiggly-line) recordings on paper-drum recorders. Eleven such recordings are produced, five of which are the proper frequencies to record some aspect of nearby earthquakes. One paper recording is produced from each of RLO, VVO, and SIO. The paper records are used as a digital system backup, and to scan for earthquakes faster than is possible on computer screens.

In addition to the digital and analog seismograms recorded at the OGS Observatory and main office, seismograms are recorded by five volunteer-operated seismographs. Each consists of a Geotech S-13 short-period vertical-motion-sensing seismometer in a shallow tank vault, or in an abandoned mine shaft (station MEO) or large-diameter, hand-dug, shallow water well (station UYO). The seismometer signal runs through 200–1,800 ft of cable in surface PVC conduit to the volunteer's house or other building. The volunteer has a Sprengnether MEQ-800B timing system amplifier-filter-drum recorder, which records 24 hours of seismic trace at 1 mm/min in a spiral path around the paper on the drum. The times are set by a time signal radio receiver tuned to the National Institute of Standards and Technology and high-frequency radio station WWV. The volunteers mail in the seismograms weekly (or more often, if requested). When an earthquake is felt in Oklahoma, the

volunteer operators fax seismogram copies to the Observatory so that the earthquake can be located rapidly.

Station OCO, which contains equipment similar to the volunteer-operated stations, is located at the Omniplex museum in Oklahoma City. Omniplex staff members change the seismic records daily as well as maintain the equipment. OGS Observatory staff help interpret the seismic data and archive the seismograms with all other Oklahoma network seismograms.

Oklahoma earthquake catalogs, earthquake maps, and related information are available on the Internet at the URL gopher://wealaka.okgeosurvey1.gov

The U.S. Geological Survey established a seismograph station 19 km from the OGS station at MEO at Meers. WMOK, the USGS station, does not record continuously. When triggered by moderately strong ground motion it transmits a short segment of data to the National Earthquake Information Service in Golden, Colorado. WMOK is used mostly for distant earthquakes, although it sometimes records some of the larger Oklahoma earthquakes. Because WMOK is so near MEO, its arrival times do not improve the accuracy of location of Oklahoma earthquakes.

Data Reduction and Archiving

Paper-recorded seismograms from short-period vertical records (SPZ) from TUL, RLO, VVO, and SIO, as well as short-period north–south (SPN), and short-period east–west (SPE) from TUL, are scanned initially for Oklahoma earthquakes. At this stage, >95% of Oklahoma earthquakes are seen.

When an Oklahoma earthquake is found on paper records, the digital system is used to analyze the SPZ, SPN, and SPE digital records from TUL, and the SPZ digital records from RLO, VVO, and SIO. This gives a preliminary location that is immediately posted on the earthquake catalog on the OGS gopher. This initial posting usually takes place within 24 hours of the earthquake's occurrence.

All digital traces are examined later in a systematic way for mainly distant earthquakes. At this stage, Oklahoma earthquakes are seen again, but few new Oklahoma earthquakes are spotted.

Near the beginning of each month, all paper records for the previous month from all stations in Oklahoma are examined. An occasional additional Oklahoma earthquake is found. All readings from the digital and paper records are then used to determine a final location. These final locations then replace the preliminary locations in the gopher catalog.

Oklahoma earthquake catalogs, earthquake maps, and related information are available on the Internet at the URL gopher://wealaka.okgeosurvey1.gov.

Earthquake Distribution

All Oklahoma earthquakes recorded on seismograms from three or more stations are located. In 1997, 117 Oklahoma earthquakes were located (Fig. 2; Table 2). Five earthquakes were reported felt (Table 3). The felt and observed effects of earthquakes generally are given values according to the Modified Mercalli intensity scale, which assigns a Roman numeral to each of 12 levels described by effects on humans, man-made constructions, or natural features (Table 4).

Two March 11 Oklahoma earthquakes were reported felt in Garvin County near Antioch. The felt areas probably were restricted to a few tens of square kilometers.

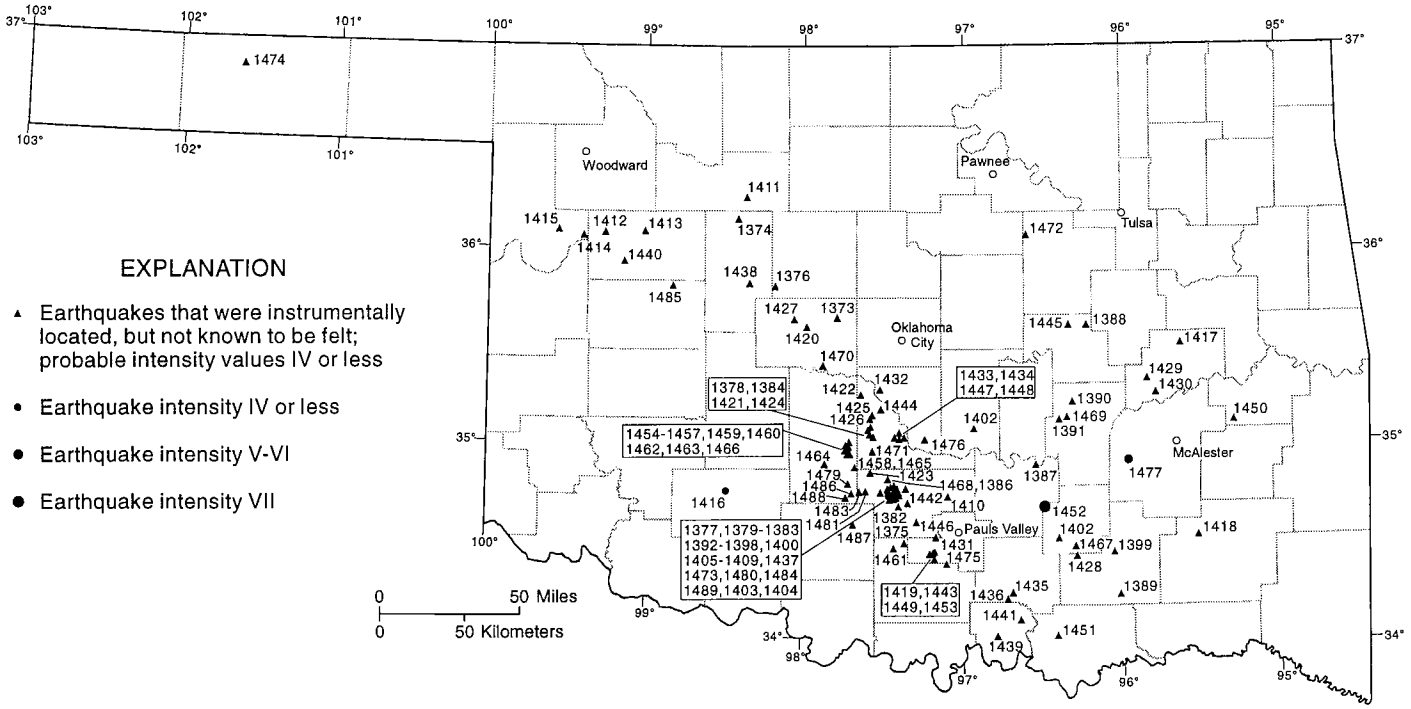

Figure 2. Distribution of Oklahoma earthquakes for 1997. Numbers correspond to event numbers in Table 2.

TABLE 2. — OKLAHOMA EARTHQUAKE CATALOG FOR 1997

Event no.	Date and origin time (UTC)[a]	County	Intensity MM[b]	Magnitudes 3Hz	Magnitudes bLg	Magnitudes DUR	Latitude deg N	Longitude deg W	Depth (km)[c]
1373	JAN 03 23 20 25.50	Canadian				2.1	35.625	97.792	5.0R
1374	JAN 10 13 55 16.77	Blaine		2.2	2.1	1.7	36.128	98.427	5.0R
1375	JAN 10 14 03 26.83	Carter		1.7		1.3	34.479	97.374	5.0R
1376	JAN 10 14 16 38.79	Kingfisher				1.3	35.786	98.195	5.0R
1377	JAN 10 14 20 16.39	Garvin		2.3	2.0	1.8	34.723	97.437	5.0R
1378	JAN 10 14 33 00.53	McClain				1.3	35.071	97.591	5.0R
1379	JAN 10 14 36 12.31	Garvin		1.9		1.5	34.735	97.446	5.0R
1380	JAN 10 14 44 18.42	Garvin		1.8		1.5	34.726	97.463	5.0R
1381	JAN 10 14 58 01.79	Garvin		2.5	2.3	1.9	34.716	97.437	5.0R
1382	JAN 10 15 17 08.40	Garvin		2.1	2.0	1.6	34.663	97.416	5.0R
1383	JAN 10 15 45 22.28	Garvin		2.2	1.9	1.7	34.765	97.432	5.0R
1384	JAN 10 16 10 51.94	McClain				1.2	35.024	97.569	5.0R
1385	JAN 10 16 51 05.74	Garvin		1.9		1.6	34.757	97.322	5.0R
1386	JAN 10 17 09 22.46	Garvin		2.3	2.2	1.8	34.804	97.479	5.0R
1387	JAN 12 19 21 07.48	Pontotoc				1.1	34.878	96.550	5.0R
1388	JAN 27 04 46 48.56	Okfuskee		1.6		1.5	35.593	96.233	5.0R
1389	FEB 05 14 18 54.74	Atoka		2.7	2.4	2.2	34.212	96.027	5.0R
1390	FEB 15 00 59 01.22	Hughes		1.9		2.1	35.196	96.319	5.0R
1391	FEB 16 11 50 48.99	Hughes		1.1		1.0	35.106	96.405	5.0R
1392	FEB 25 15 42 15.58	Garvin		1.8		1.3	34.725	97.443	5.0R
1393	FEB 25 16 00 13.62	Garvin		2.1	2.0	1.7	34.716	97.452	5.0R
1394	FEB 25 16 31 52.25	Garvin		1.7		1.0	34.720	97.411	5.0R
1395	FEB 25 16 45 11.35	Garvin		2.0	1.8	1.7	34.700	97.443	5.0R
1396	FEB 25 17 00 34.37	Garvin		1.8		1.5	34.723	97.445	5.0R
1397	FEB 25 18 01 21.25	Garvin		2.2	2.2	1.8	34.700	97.450	5.0R
1398	FEB 25 19 39 49.81	Garvin		2.1	2.0	1.6	34.721	97.435	5.0R
1399	FEB 26 00 50 52.89	Atoka				1.7	34.426	96.062	5.0R
1400	FEB 27 23 01 24.41	Garvin				1.9	34.731	97.421	5.0R
1401	FEB 27 23 45 56.65	Pottawatomie				1.7	35.063	96.945	5.0R
1402	MAR 05 10 50 18.49	Coal				1.3	34.497	96.409	5.0R
1403	MAR 11 13 30 32.22	Garvin	3	2.6	2.5	2.2	34.743	97.484	5.0R
1404	MAR 11 13 43 59.89	Garvin	2			2.1	34.725	97.415	5.0R
1405	MAR 11 14 34 33.79	Garvin				1.6	34.759	97.472	5.0R
1406	MAR 11 14 35 32.40	Garvin				1.4	34.731	97.472	5.0R
1407	MAR 11 14 48 37.15	Garvin				1.7	34.743	97.443	5.0R
1408	MAR 11 15 13 43.98	Garvin				2.0	34.731	97.437	5.0R
1409	MAR 11 15 47 15.35	Garvin				2.0	34.747	97.452	5.0R
1410	MAR 11 17 09 20.55	Garvin				1.4	34.708	97.120	5.0R
1411	MAR 21 21 31 44.58	Major				1.8	36.238	98.373	5.0R
1412	MAR 21 21 45 07.58	Dewey				1.9	36.054	99.271	5.0R
1413	MAR 21 22 09 00.00	Dewey				1.7	36.074	99.021	5.0R
1414	MAR 21 23 47 20.50	Ellis		2.4	2.2	2.4	36.042	99.396	5.0R
1415	MAR 22 06 27 39.99	Ellis				1.7	36.074	99.568	5.0R
1416	APR 20 10 02 30.63	Comanche	3	1.8	2.0	2.0	34.743	98.483	5.0R
1417	MAY 07 16 59 21.15	McIntosh				1.6	35.493	95.632	5.0R
1418	MAY 16 02 16 15.52	Pushmataha		1.4		1.7	34.509	95.534	5.0R
1419	MAY 17 00 55 19.88	Murray				1.8	34.395	97.187	5.0R
1420	MAY 23 17 57 42.97	Canadian				1.8	35.580	97.991	5.0R
1421	MAY 23 18 32 51.84	McClain				1.8	35.053	97.604	5.0R
1422	MAY 23 18 46 20.27	McClain				1.6	35.231	97.657	5.0R
1423	MAY 23 18 57 45.93	Garvin				2.0	34.846	97.585	5.0R
1424	MAY 23 19 08 47.99	McClain				1.4	35.028	97.585	5.0R
1425	MAY 23 19 41 08.88	McClain				2.1	35.121	97.585	5.0R
1426	MAY 23 20 50 43.18	McClain				1.9	35.127	97.581	5.0R
1427	MAY 23 21 10 07.78	Canadian				2.0	35.619	98.069	5.0R
1428	JUN 07 09 04 10.53	Atoka		2.0	1.7	2.0	34.411	96.296	5.0R
1429	JUN 08 11 21 07.69	McIntosh				1.4	35.319	95.847	5.0R
1430	JUN 09 11 20 59.49	McIntosh		1.6		1.4	35.243	95.792	5.0R
1431	JUN 11 00 21 21.83	Murray				1.7	34.505	97.159	5.0R
1432	JUN 15 23 21 01.65	Cleveland		1.9	1.8	1.9	35.260	97.531	5.0R
1433	JUN 16 00 40 45.95	McClain		2.3	2.0	1.7	35.012	97.406	5.0R
1434	JUN 16 02 48 00.06	McClain		1.8	1.8	1.8	35.020	97.374	5.0R

Event no.	Date and origin time (UTC)[a]	County	Intensity MM[b]	Magnitudes 3Hz	bLg	DUR	Latitude deg N	Longitude deg W	Depth (km)[c]
1435	JUN 23 04 36 35.59	Johnston		1.6		1.5	34.223	96.702	5.0R
1436	JUN 23 05 20 49.85	Johnston		1.7	1.6	1.5	34.192	96.726	5.0R
1437	JUN 28 15 54 48.54	Garvin		2.6	2.2	2.2	34.696	97.468	5.0R
1438	JUL 07 06 51 46.10	Blaine				1.9	35.799	98.350	5.0R
1439	JUL 07 08 52 03.00	Marshall		1.8	2.3	1.7	33.997	96.796	5.0R
1440	JUL 07 11 36 19.06	Dewey				1.9	35.917	99.146	5.0R
1441	JUL 14 10 43 47.45	Marshall		1.8	1.9	1.5	34.083	96.656	5.0R
1442	JUL 18 19 08 38.74	Garvin		2.3	2.2	2.0	34.678	97.363	5.0R
1443	JUL 26 00 46 46.09	Murray		1.4	1.7	1.7	34.432	97.175	5.0R
1444	AUG 02 01 47 59.03	McClain		1.5	1.7	1.4	35.156	97.526	5.0R
1445	AUG 04 14 15 26.28	Okfuskee				1.8	35.589	96.346	5.0R
1446	AUG 05 00 37 07.68	Garvin		1.2		1.8	34.581	97.302	5.0R
1447	AUG 10 14 12 59.16	McClain		2.5		2.0	35.038	97.408	5.0R
1448	AUG 16 00 20 27.85	McClain				2.1	35.015	97.424	5.0R
1449	AUG 16 16 40 53.00	Murray				1.9	34.419	97.210	5.0R
1450	AUG 23 09 10 35.22	Haskell				2.6	35.095	95.300	5.0R
1451	AUG 29 05 22 38.52	Bryan		1.9		1.7	34.005	96.421	5.0R
1452	SEP 06 23 38 01.99	Coal	7		4.4	3.7	34.676	96.499	5.0R
1453	SEP 12 19 31 55.86	Murray				1.6	34.424	97.194	5.0R
1454	SEP 18 12 32 02.94	Grady		1.8		1.8	34.929	97.713	5.0R
1455	SEP 18 12 46 44.25	Grady				1.7	34.986	97.725	5.0R
1456	SEP 18 13 32 06.39	Grady				1.9	34.966	97.734	5.0R
1457	SEP 18 13 10 41.45	Grady				1.6	34.952	97.737	5.0R
1458	SEP 18 13 13 09.03	Grady				1.5	34.861	97.687	5.0R
1459	SEP 18 13 53 18.04	Grady				1.9	34.966	97.741	5.0R
1460	SEP 18 14 24 44.13	Grady				1.8	34.929	97.713	5.0R
1461	SEP 18 14 48 15.64	Carter				1.8	34.451	97.444	5.0R
1462	SEP 18 15 01 03.63	Grady		2.1	1.8	1.7	34.944	97.749	5.0R
1463	SEP 18 15 31 09.91	Grady		1.8		1.7	34.929	97.721	5.0R
1464	SEP 18 15 59 42.66	Grady		1.9		1.8	34.876	97.873	5.0R
1465	SEP 18 17 40 52.64	Grady		2.3	2.4	2.0	34.861	97.687	5.0R
1466	SEP 18 20 11 18.63	Grady		2.0	1.8	1.7	34.952	97.737	5.0R
1467	SEP 18 15 06 46.61	Coal				1.8	34.462	96.304	5.0R
1468	OCT 12 07 21 53.66	Garvin				2.0	34.809	97.538	5.0R
1469	OCT 14 05 07 40.36	Huges				1.9	35.122	96.351	5.0R
1470	OCT 23 02 06 08.72	Canadian				1.7	35.382	97.885	5.0R
1471	OCT 23 03 35 13.53	McClain				1.7	34.945	97.559	5.0R
1472	NOV 02 07 08 56.69	Creek				1.5	36.039	96.612	5.0R
1473	NOV 04 17 01 11.25	Garvin		2.0	1.8	1.9	34.731	97.538	5.0R
1474	NOV 14 11 25 32.72	Texas				2.4	36.863	101.625	5.0R
1475	NOV 21 20 57 59.11	Carter				1.9	34.372	97.109	5.0R
1476	DEC 03 23 35 34.79	Cleveland				1.4	35.007	97.244	5.0R
1477	DEC 06 11 11 23.61	Pittsburg	4	2.9	2.8	2.7	34.895	95.968	5.0R
1478	DEC 10 08 50 35.28	Garvin		2.0	2.0	1.7	34.735	97.452	5.0R
1479	DEC 20 01 40 32.48	Grady		1.6	1.4	1.5	34.774	97.731	5.0R
1480	DEC 20 13 18 43.56	Garvin		2.0	1.8	1.7	34.731	97.451	5.0R
1481	DEC 20 13 28 27.85	Garvin		1.4		1.6	34.731	97.663	5.0R
1482	DEC 20 13 30 14.35	Garvin		1.2			34.704	97.404	5.0R
1483	DEC 20 13 36 30.56	Garvin		2.0		1.6	34.735	97.616	5.0R
1484	DEC 20 13 52 11.38	Garvin		1.8	1.8	1.6	34.751	97.472	5.0R
1485	DEC 21 16 58 42.50	Custer				1.5	35.784	98.835	5.0R
1486	DEC 21 17 27 49.10	Grady				1.4	34.729	97.704	5.0R
1487	DEC 22 00 59 51.72	Stephens				1.8	34.569	97.698	5.0R
1488	DEC 23 09 07 14.75	Grady				1.6	34.708	97.738	5.0R
1489	DEC 24 02 33 10.88	Garvin		1.8	1.7	1.6	34.755	97.468	5.0R

[a]UTC refers to Coordinated Universal Time, formerly Greenwich Mean Time. The first two digits refer to the hour on a 24-hour clock. The next two digits refer to the minute, and the remaining digits are the second. To convert to local Central Standard Time, subtract 6 hours.

[b]Modified Mercalli (MM) earthquake-intensity scale (see Table 4).

[c]The hypocenter is restrained (R) at an arbitrary depth of 5.0 km, except where indicated, for purposes of computing latitude, longitude, and origin time.

TABLE 3. — EARTHQUAKES REPORTED FELT IN OKLAHOMA, 1997

Event no.	Date and origin time (UTC)[a]	Nearest city	County	Intensity MM[b]
1403	MAR 11 13 30 32.22	7 km NW of Antioch	Garvin	3
1404	MAR 11 13 43 59.89	Antioch	Garvin	2
1416	APR 20 10 02 30.63	Medicine Park	Comanche	3
1452	SEP 06 23 38 01.99	3 km NE of Stonewall	Coal	7
1477	DEC 06 11 11 23.61	Haywood	Pittsburg	4

[a]UTC refers to Coordinated Universal Time, formerly Greenwich Mean Time. The first two digits refer to the hour on a 24-hour clock. The next two digits refer to the minute, and the remaining digits are the second. To convert to local Central Standard Time, subtract 6 hours.

[b]Modified Mercalli (MM) earthquake-intensity scale (see Table 4).

On April 20, 1997, a small earthquake was reported felt near Medicine Park, Comanche County. At 1:23 a.m., September 6 (local time and date), a magnitude-4.4 (mbLg) earthquake occurred 3 km northeast of Stonewall in Coal County. This earthquake, the third largest to have occurred in Oklahoma in this century, produced MM-VII effects near the epicenter and had an approximate 48,109-km^2 felt area. The earthquake was reported felt in Tulsa, Durant, Oklahoma City, Stillwater, and several other places.

A magnitude-2.8 (mbLg) earthquake was reported felt in Haywood, Arpealar, Stuart, Ashland, Kiowa, and McAlester. This earthquake, which produced MM-IV effects near the epicenter, had an approximate 155-km^2 felt area.

Earthquake-magnitude values ranged from a low of 1.0 (MDUR) in Hughes County to a high of 4.4 (mbLg) in Coal County. More than half (64) of the 1997 locatable earthquakes occurred in Garvin, Grady, and McClain Counties. Five earthquakes were located in Murray County; four earthquakes were located in Canadian County; three earthquakes were located in Carter, Coal, Hughes, Pittsburg, McIntosh, and Dewey Counties.

Catalog

A desktop computer system, including linked HP-9825T and HP-9835A computers, hard and flexible disks, and printers, is used to calculate and catalog local earthquake epicenters. Any earthquake within Oklahoma or within about 100–200 km of Oklahoma's borders is considered a local earthquake. A catalog containing date, origin time, county, intensity, magnitude, location, focal depth, and references is printed in page-sized format. This catalog is maintained in addition to the gopher catalog of earthquakes only in Oklahoma. Table 2 contains 1997 Oklahoma earthquake data displayed in a modified version of the regional earthquake catalog. Each event is sequentially numbered and arranged according to date and origin time. The numbering system is compatible with the system used by Lawson and Luza (1980–90, 1993–97), Lawson and others (1991,1992), and for the *Earthquake Map of Oklahoma* (Lawson and Luza, 1995b).

The date and time are given in UTC. UTC refers to Coordinated Universal Time, formerly Greenwich Mean Time. The first two digits refer to the hour on a 24-hour

TABLE 4. — MODIFIED MERCALLI (MM) EARTHQUAKE-INTENSITY SCALE
(Abridged) (Modified from Wood and Neumann, 1931)

I	Not felt except by a very few under especially favorable circumstances.
II	Felt only by a few persons at rest, especially on upper floors of buildings. Suspended objects may swing.
III	Felt quite noticeably indoors, especially on upper floors of buildings. Automobiles may rock slightly.
IV	During the day felt indoors by many, outdoors by few. At night some awakened. Dishes, doors, windows disturbed. Automobiles rocked noticeably.
V	Felt by nearly everyone, many awakened. Some dishes, windows, etc., broken; unstable objects overturned. Pendulum clocks may stop.
VI	Felt by all; many frightened and run outdoors.
VII	Everybody runs outdoors. Damage negligible in buildings of good design and construction. Shock noticed by persons driving automobiles.
VIII	Damage slight in specially designed structures; considerable in ordinary substantial buildings; great in poorly built structures. Fall of chimneys, stacks, columns. Persons driving automobiles disturbed.
IX	Damaged considerable even in specially designed structures; well-designed frame structures thrown out of plumb. Buildings shifted off foundations. Ground cracked conspicuously.
X	Some well-built wooden structures destroyed; ground badly cracked, rails bent. Landslides and shifting of sand and mud.
XI	Few if any (masonry) structures remain standing. Broad fissures in ground.
XII	Damage total. Waves seen on ground surfaces.

clock. The next two digits refer to the minute, and the remaining digits are the seconds. To convert to local Central Standard Time, subtract 6 hours.

Earthquake magnitude is a measurement of energy and is based on data from seismograph records. The magnitude of a local earthquake is determined by taking the logarithm (base 10) of the largest ground motion recorded during the arrival of a seismic-wave type and applying a standard correction for distance to the epicenter. When the magnitude value is increased one unit, the amplitude of the earthquake waves increases 10 times. There are several different scales used to report magnitude. Table 2 has three magnitude scales, which are mbLg (Nuttli), m3Hz (Nuttli), and MDUR (Lawson). Each magnitude scale was established to accommodate specific criteria, such as the distance from the epicenter, as well as the availability of certain seismic data.

For earthquake epicenters located 11–222 km from a seismograph station, Otto Nuttli developed the m3Hz magnitude scale (Zollweg, 1974). This magnitude is derived from the following expression:

$$m3Hz = \log(A/T) - 1.63 + 0.87 \log(\Delta),$$

where A is the maximum center-to-peak vertical-ground-motion amplitude sustained for three or more cycles of Lg waves, near 3 Hz in frequency, measured in nanometers; T is the period of the Lg waves measured in seconds; and Δ is the great-circle distance from epicenter to station measured in kilometers.

In 1979, St. Louis University (Stauder and others, 1979) modified the formulas for m3Hz. This modification was used by the OGS Observatory beginning January 1, 1982. The modified formulas had the advantage of extending the distance range for measurement of m3Hz out to 400 km, but also had the disadvantage of increasing m3Hz by about 0.12 units compared to the previous formula. Their formulas were given in terms of $\log(A)$ but were restricted to wave periods of 0.2–0.5 sec. In order to use $\log(A/T)$, we assumed a period of 0.35 sec in converting the formulas for our use. The resulting equations are:

(epicenter 10–100 km from a seismograph)

$$\text{m3Hz} = \log(A/T) - 1.46 + 0.88 \log(\Delta)$$

(epicenter 100–200 km from a seismograph)

$$\text{m3Hz} = \log(A/T) - 1.82 + 1.06 \log(\Delta)$$

(epicenter 200–400 km from a seismograph)

$$\text{m3Hz} = \log(A/T) - 2.35 + 1.29 \log(\Delta).$$

Otto Nuttli's (1973) earthquake magnitude, mbLg, for seismograph stations located between 55.6 and 445 km from the epicenter, is derived from the following equation:

$$\text{mbLg} = \log(A/T) - 1.09 + 0.90 \log(\Delta).$$

Where seismograph stations are located between 445 and 3,360 km from the epicenter, mbLg is defined as:

$$\text{mbLg} = \log(A/T) - 3.10 + 1.66 \log(\Delta),$$

where A is the maximum center-to-peak vertical-ground-motion amplitude sustained for three or more cycles of Lg waves, near 1 Hz in frequency, measured in nanometers; T is the period of Lg waves measured in seconds; and Δ is the great-circle distance from epicenter to station measured in kilometers.

The MDUR magnitude scale was developed by Lawson (1978) for earthquakes in Oklahoma and adjacent areas. It is defined as:

$$\text{MDUR} = 1.86 \log(\text{DUR}) - 1.49,$$

where DUR is the duration or difference, in seconds, between the Pg-wave arrival time and the time the final coda amplitude decreases to twice the background-noise amplitude. Before 1981, if the Pn wave was the first arrival, the interval between the earthquake-origin time and the decrease of the coda to twice the background-noise amplitude was measured instead. Beginning January 1, 1982, the interval from the beginning of the P wave (whether it was Pg, P*, or Pn) to the decrease of the coda to twice the background-noise amplitude was used.

The depth to the earthquake hypocenter is measured in kilometers. For most Oklahoma earthquakes the focal depth is unknown. In almost all Oklahoma events, the stations are several times farther from the epicenter than the likely depth of the event. This makes the locations indeterminate at depth, which usually requires that the hypocenter depth be restrained to an arbitrary 5 km for purposes of computing latitude, longitude, and origin time. All available evidence indicates that no Oklahoma hypocenters have been deeper than 15–20 km.

Earthquake detection and location accuracy have been greatly improved since the installation of the statewide network of seismograph stations. The frequency of earthquake events and the possible correlation of earthquakes to specific tectonic elements in Oklahoma are being studied. It is hoped that this information will provide a more complete data base that can be used to develop numerical estimates of earthquake risk, giving the approximate frequency of the earthquakes of any given size for various regions of Oklahoma. Numerical risk estimates could be used for better design of large-scale structures, such as dams, high-rise buildings, and power plants, as well as to provide the necessary information to evaluate insurance rates.

Acknowledgments

Shirley Jackson, Todd McCormick, and John Humphrey maintained the OGS Observatory at Leonard. Volunteer seismograph-station operators and landowners at various locations in Oklahoma make possible the operation of a statewide seismic network.

This work was funded directly by the Oklahoma Geological Survey. The GSE digital seismic system, provided by the Defense Advanced Research Projects Agency/Nuclear Monitoring Research Office, considerably enhanced the OGS's ability to analyze Oklahoma earthquakes. A borehole seismic system, a joint project with the Lawrence Livermore National Laboratories, was useful in recording Oklahoma earthquakes. The Observatory exists because of building and land-purchase gifts from Jersey Production Research Co. (now merged into Exxon) and the Sarkeys Foundation.

References Cited

Docekal, Jerry, 1970, Earthquakes of the stable interior, with emphasis on the Midcontinent: University of Nebraska, Lincoln, unpublished Ph.D. dissertation, v. 1, 169 p.; v. 2, 332 p.

Indian Pioneer Papers [date unknown], Interview, Eliza Ross: Western History Collections, University of Oklahoma Libraries, Norman, v. 78, p. 164–167.

Kalb, Bill, 1964, Earthquakes that shook Oklahoma: Orbit Magazine—The Sunday Oklahoman, Oklahoma City, September 27, p. 4–7.

Lawson, J. E., Jr., 1978, A preliminary duration magnitude scale for local and regional earthquakes recorded at Oklahoma seismograph stations: Oklahoma Geological Survey Observatory Open-File Report, 14 p.

_____ 1980, Geophysical observatory establishes continuous time synchronization: Oklahoma Geology Notes, v. 40, p. 214.

Lawson, J. E., Jr.; and Luza, K. V., 1980, Oklahoma earthquakes, 1979: Oklahoma Geology Notes, v. 40, p. 95–105.

_____ 1981, Oklahoma earthquakes, 1980: Oklahoma Geology Notes, v. 41, p. 140–149.

_____ 1982, Oklahoma earthquakes, 1981: Oklahoma Geology Notes, v. 42, p. 126–137.

_____ 1983, Oklahoma earthquakes, 1982: Oklahoma Geology Notes, v. 43, p. 24–35.

_____ 1984, Oklahoma earthquakes, 1983: Oklahoma Geology Notes, v. 44, p. 32–42.

_____ 1985, Oklahoma earthquakes, 1984: Oklahoma Geology Notes, v. 45, p. 52–61.

_____ 1986, Oklahoma earthquakes, 1985: Oklahoma Geology Notes, v. 46, p. 44–52.

_____ 1987, Oklahoma earthquakes, 1986: Oklahoma Geology Notes, v. 47, p. 65–72.

_____ 1988, Oklahoma earthquakes, 1987: Oklahoma Geology Notes, v. 48, p. 54–63.

_____ 1989, Oklahoma earthquakes, 1988: Oklahoma Geology Notes, v. 49, p. 40–48.

_____ 1990, Oklahoma earthquakes, 1989: Oklahoma Geology Notes, v. 50, p. 68–76.

_____ 1993, Oklahoma earthquakes, 1992: Oklahoma Geology Notes, v. 53, p. 51–62.
_____ 1994, Oklahoma earthquakes, 1993: Oklahoma Geology Notes, v. 54, p. 57–68.
_____ 1995a, Oklahoma earthquakes, 1994: Oklahoma Geology Notes, v. 55, p. 51–63.
_____ 1995b, Earthquake map of Oklahoma (earthquakes shown through 1993): Oklahoma Geological Survey Map GM-35, scale 1:500,000.
_____ 1996, Oklahoma earthquakes, 1995: Oklahoma Geology Notes, v. 56, p. 49–63.
_____ 1997, Oklahoma earthquakes, 1996: Oklahoma Geology Notes, v. 57, p. 40–52.

Lawson, J. E., Jr.; Luza, K. V.; and Moss, Dan, 1991, Oklahoma earthquakes, 1990: Oklahoma Geology Notes, v. 51, p. 50–61.

Lawson, J. E., Jr.; Luza, K. V.; Brown, R. L.; and Moss, Dan, 1992, Oklahoma earthquakes, 1991: Oklahoma Geology Notes, v. 52, p. 48–59.

Luza, K. V., 1978, Regional seismic and geologic evaluations of Nemaha uplift, Oklahoma, Kansas, and Nebraska: Oklahoma Geology Notes, v. 38, p. 49–58.

Mykkeltveit, Svein; Ringdal, Frode; Kvaerna, Tormad; and Alewine, R. W., 1990, Application of regional arrays in seismic verification: Seismological Society of America Bulletin, v. 80, p. 1777–1801.

Nuttli, O. W., 1973, Seismic wave attenuation and magnitude relations for eastern North America: Journal of Geophysical Research, v. 78, p. 876–885.

Ross, D. H. (ed.), 1882, Shake: Cherokee Advocate, Friday, October 27, p. 1.

Stauder, W.; Hermann, R.; Singh, S.; Reidy, D.; Perry, R.; and Morrissey, Sean-Thomas, 1979, Central Mississippi Valley Earthquake Bulletin: First Quarter 1979, no. 19, 50 p.

Stover, C. W.; Reagor, B. G.; Algermissen, S. T.; and Lawson, J. E., Jr., 1981, Seismicity map of the State of Oklahoma: U.S. Geological Survey Miscellaneous Field Studies Map MF-1352, scale 1:1,000,000.

Tarbuck, E. J.; and Lutgens, F. K., 1990, The earth—an introduction to physical geology: Merrill Publishing Co., Columbus, Ohio, 651 p.

von Hake, C. A., 1976, Earthquake history of Oklahoma: Earthquake Information Bulletin, v. 8, p. 28–30.

Wells, L. L., 1975, Young Cushing in Oklahoma Territory: Frontier Printers, Stillwater, Oklahoma, 221 p.

Wood, H. O.; and Neumann, Frank, 1931, Modified Mercalli intensity scale of 1931: Seismological Society of America Bulletin, v. 21, p. 227–283.

Zollweg, James, 1974, A preliminary study of the seismicity of the central United States, 1974: St. Louis University unpublished undergraduate report, 15 p.

Notes on New Publications

Digital Seismic Recordings of the May 23, 1995, Demolition of the Alfred P. Murrah Federal Building, Oklahoma City, Oklahoma

C. M. Dietel is the author of this 14-page USGS open-file report.

Order OF 95-0594 from: U.S. Geological Survey, Information Services, Box 25286, Denver Federal Center, Denver, CO 80225; telephone (303) 202-4210. Cost is $2.50 for a paper copy or $4 for microfiche, plus $3.50 per order for handling.

Techniques for Estimating Peak-Streamflow Frequency for Unregulated Streams and Streams Regulated by Small Floodwater Retarding Structures in Oklahoma

Presented in this 39-page report are techniques for estimating the peak discharge and flood frequency (peak-streamflow frequency) for selected recurrence intervals from 2 to 500 years for ungaged sites on natural unregulated streams with drainage areas <2,510 mi^2 in Oklahoma. The report also provides techniques for estimating peak-streamflow frequency for gaged sites on natural unregulated streams and using the result to estimate nearby ungaged sites on the same stream. Lastly, it provides procedures to adjust estimates for ungaged urban basins and basins regulated by floodwater-retarding structures. The study updated regression equations for estimating the peak-stramflow frequency of floods for Oklahoma streams with a drainage area <2,510 mi^2. It was conducted by the U.S. Geological Survey in cooperation with the Oklahoma Department of Transportation; the report author is Robert L. Tortorelli. A companion report is described below.

Order WRI 97-4202 from: U.S. Geological Survey, Water Resources Division, 202 N.W. 66th St., Bldg. 7, Oklahoma City, OK 73116; phone (405) 843-7570. A limited number of copies are available free of charge.

Digital Map Grids of Mean-Annual Precipitation for 1961–90, and Generalized Skew Coefficients of Annual Maximum Streamflow for Oklahoma

Digital data suitable for use with geographic information systems software are provided in this U.S. Geological Survey open-file report, a companion report to USGS WRI Report 97-4202 (see previous description). The digital report contains two digital-map grids of data that were used to develop peak-flow regression equations for Oklahoma. One data set is a grid of mean annual precipitation, in inches, based on the period 1961–90; these data are required as input for the regression equations. The second data set is a grid of generalized skew coefficients of logarithms of annual maximum streamflow for Oklahoma streams ≤2,510 mi^2 in drainage area; the data are used to compute flood-frequency statistics for stream sites with streamflow data.

Order OF 97-574 from: U.S. Geological Survey, Water Resources Division, 202 N.W. 66th St., Bldg. 7, Oklahoma City, OK 73116; phone (405) 843-7570. A limited number of copies are available free of charge.

NEW OGS *Publications*

CIRCULAR 99. ***Simpson and Viola Groups in the Southern Midcontinent, 1994 Symposium,*** edited by Kenneth S. Johnson. 275 pages, 30 contributions. Price: Paperbound, $12.

From the editor's preface:

The transfer of technical information will aid in the search for, and production of, our oil and gas resources. To facilitate this technology transfer, the Oklahoma Geological Survey (OGS) and the Bartlesville Project Office of the U.S. Department of Energy (BPO–DOE) co-sponsored a symposium dealing with petroleum geology and reservoir characterization of the Simpson and Viola Groups in the southern Midcontinent. The symposium was held March 29–30, 1994, at the Oklahoma Center for Continuing Education, The University of Oklahoma, Norman. This volume contains the proceedings of that symposium.

Research reported upon at the symposium focused on geology, depositional settings, reservoir characterization, diagenetic history, enhanced oil recovery, and horizontal drilling. In describing the various petroleum reservoirs in the Simpson and Viola Groups in the southern Midcontinent, the researchers have increased our understanding of how the depositional and diagenetic history of these strata can affect reservoir heterogeneity and our ability to efficiently recover the hydrocarbons they contain. We hope that the symposium and these proceedings will bring such research to the attention of the geoscience and energy-research community, and will help foster exchange of information and increased research interest among industry, university, and government workers.

Twenty papers were presented orally at the symposium, and they are presented in this volume as full papers or abstracts. An additional 10 reports were given as posters, and they are presented as short reports or abstracts. About 280 persons attended the symposium. Stratigraphic nomenclature and age determinations used by the various authors in this volume do not necessarily agree with those of the OGS.

This is the seventh symposium in as many years dealing with topics of major interest to geologists and others involved in petroleum-resource development in Oklahoma and adjacent states. These symposia are intended to foster the exchange of information that will improve our ability to find and recover our nation's oil and gas resources. Earlier symposia subjects covered the Anadarko basin (published as OGS Circular 90); Late Cambrian–Ordovician geology of the southern Midcontinent (OGS Circular 92); source rocks in the southern Midcontinent (OGS Circular 93); petroleum-reservoir geology in the southern Midcontinent (OGS Circular 95); structural styles in the southern Midcontinent (OGS Circular 97); and deltaic reservoirs in the southern Midcontinent (OGS Circular 98).

SPECIAL PUBLICATION 98-1. ***Petroleum Core Catalog, Oklahoma Geological Survey—April 1998,*** compiled by Water C. Esry and Larry T. Austin. 212 pages. Price: $10 for paper copy; data also available on 3.5-in. floppy disks for $10.

Listed in this catalog are the petroleum cores, the largest and most-used group of materials contained in the OGS Core and Sample Library. The Library, established

in 1936 by Robert H. Dott, former director of the OGS, is used by petroleum company personnel, geoscientists, and students throughout the United States.

The petroleum group consists of cores from more than 4,100 wells drilled in Oklahoma, contained in an estimated 79,235 boxes. This information has been computerized and incorporated in the Natural Resources Information System (NRIS) of Oklahoma, which is a group of interrelated data bases that together provide a wide range of information on the State's oil and gas resources. NRIS is being constructed to respond to the growing need for access to information on the State's natural resources.

The petroleum core data base presented in this catalog consists of information on section, township, range, well location, county, operator, well name and number, formation name, cored depth interval, "catalog" interval number, number of boxes, diameter of the core, condition, representation, total feet cored, average feet per box, and the library file number.

Although not included in the Petroelum Core Catalog, the Library also contains samples (well cuttings) and nonpetroleum cores related to coal, minerals, and special stratigraphic studies. These items are listed in a separate card file at the Library.

SPECIAL PUBLICATION 98-2. ***Coal Geology of Muskogee County, Oklahoma,*** by LeRoy A. Hemish. 111 pages, 3 plates. Price: $12.

Author's abstract:

Muskogee County is located in the east-central part of the coal belt of eastern Oklahoma. Coal-bearing strata of Desmoinesian (Middle Pennsylvanian) age underlie ~500 mi^2 in the western two-thirds of the county. Remaining resources of coal in the area total 95,557,000 tons (all tonnage figures are in short tons), and reserves total 11,141,000 tons.

Tonnage figures for estimated resources and reserves show a significant increase for Muskogee County, resulting from new data, detailed mapping, and new exploratory work. Ten coal beds in Muskogee County have commercial potential: Hartshorne coal, with reserves of 59,000 tons; Keefton coal, 624,000 tons; Stigler coal, 3,006,000 tons; Spaniard coal, 60,000 tons; Rowe coal, 751,000 tons; Secor coal, 815,000 tons; Peters Chapel coal, 3,192,000 tons; Wainwright coal, 1,823,000 tons; Tebo coal, 794,000 tons; and Croweburg coal, 17,000 tons.

Coals of the area are predominantly of high-volatile A bituminous (hvAb) rank. The Hartshorne, Keefton, and Secor coals have much lower sulfur content than the others, averaging ~1.1%. The combined average sulfur content of all the other coals is ~5.0%.

In the late 1980s and early 1990s, one mine operator was producing coal from the Secor bed in Muskogee County. Another operator was mining the Keefton coal until the mine was closed in 1993. Surface-mining methods were used in both operations. At the time of this writing (1994) no coal is being produced in Muskogee County.

OGS Circular 100, SP 98-1, and SP 98-2 can be purchased by mail from the Survey at 100 E. Boyd, Room N-131, Norman, OK 73019; fax 405-325-7069. To mail order, add 20% to the cost for postage, with a minimum of $1 per order.

All OGS publications can be purchased over the counter at the OGS Publication Sales Office, 1218-B W. Rock Creek Road, Norman; phone (405) 360-2886, fax 405-366-2882.

OGS Holds Workshop on Waterflooding

The Oklahoma Geological Survey will present a one-day workshop, "Geological Considerations of Waterflooding," on June 10 and 11, 1998, at the Francis Tuttle Vo-Tech, 12777 N. Rockwell, Oklahoma City. On both days the workshop starts at 9 a.m. and ends at 4 p.m.

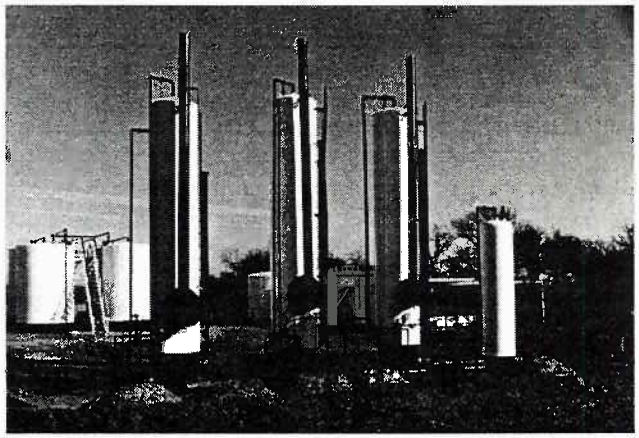

Portion of a central tank battery facility located in east-central Oklahoma.

The aim of the workshop is to acquaint geologists and engineers with the hazards that can jeopardize the potential success of a waterflood candidate. The program will address the following topics:

- determining reservoir data;
- deciphering production data;
- determining and isopaching net pay;
- sand geometry boundaries;
- coring and core results;
- distinguishing natural and induced fractures;
- water supply evaluation;
- permitting.

The workshop represents part of the Survey's ongoing effort to help geologists broaden their knowledge of various geologic subjects through seminars, workshops, and publications.

"Today's economic climate and trend toward downsizing forces companies to require geologists and engineers to familiarize themselves with subjects other than their own specialty. The OGS recognizes this scenario," says Kurt Rottmann, the coordinator of the program and principal presenter.

Rottmann, a consultant geologist based in Oklahoma City, contributed to several of the workshops on fluvial-dominated deltaic oil reservoirs held by the OGS from 1995 to 1997.

Assisting Rottmann will be David R. Crutchfield, consultant petroleum reservoir engineer, Oklahoma City; and Saleem Nizami, APEC, Inc., Oklahoma City.

The registration fee for the workshop is $30. The cost includes coffee, lunch, and a copy of the workshop publication, *Geological Considerations of Waterflooding* (OGS Special Publication 98-3).

For more details, or for registration forms, contact Michelle Summers, Oklahoma Geological Survey, 100 E. Boyd, Room N-131, Norman, OK 73019; (405) 325-3031 or (800) 330-3996; fax 405-325-7069.

UPCOMING *Meetings*

Geological Society of America, Rocky Mountain Section Annual Meeting, May 25–26, 1998, Flagstaff, Arizona. Information: Larry Middleton, Dept. of Geology, Box 4099, Northern Arizona University, Flagstaff, AZ 86011; (520) 523-2429; e-mail: Larry.Middleton@nau.edu.

U.S. National Conference on Earthquake Engineering: Seismic Design and Mitigation for the Third Millenium, May 31–June 4, 1998, Seattle, Washington. Information: Earthquake Engineering Research Institute, 499 14th St., Suite 320, Oakland, CA 94612; (510) 451-0905, fax 510-451-5411; e-mail: eeri@eeri.org.

Integrated Technical Approaches to Site Characterization, June 8–10, 1998, Chicago, Illinois. Information: Lorraine M. LaFreniere, Argonne National Laboratory, 9700 South Cass Ave., Bldg. 203, Argonne, IL 60439; (630) 252-7969, fax 630-252-5747; e-mail: ITASC@anl.gov; World Wide Web: http://www.anl.gov/ITASC.

National Minerals Education Conference, June 17–20, 1998, Pittsburgh, Pennsylvania. Information: Marianne Miller, P.O. Box 18070, Cochrans Mill Road, Pittsburgh, PA 15236; (412) 892-6786, fax 412-892-4288; e-mail: zka7@cdc.gov.

Interstate Oil and Gas Compact Commission, Midyear Meeting, June 21–23, 1997, Overland Park, Kansas. Information: Interstate Oil and Gas Compact Commission, P.O. Box 53127, Oklahoma City, OK 73152; (405) 525-3556, fax 405-525-3592; e-mail: iogcc@oklaosf.state.ok.us.

Society of Independent Professional Earth Scientists, July 22–24, 1998, Durango, Colorado. Information: SIPES, 4925 Greenville Ave., Suite 1106, Dallas, TX 75206; (214) 363-1780; e-mail: sipes@sipes.org.

International Mineralogical Association Meeting, August 9–15, 1998, Toronto, Ontario. Information: A. J. Naldrett, Dept. of Geology, University of Toronto, Toronto, Ontario M5S 3B1, Canada; (416) 978-3030, fax 416-978-3938; e-mail: ima98@ quartz.geology.utoronto.ca.

Hartshorne Play Workshop, September 30, 1998, Oklahoma City, Oklahoma, and November 4, 1998, Muskogee, Oklahoma; and **Hartshorne Play Field Trip,** November 11–12, 1998, Muskogee, Oklahoma. Information: Michelle Summers, Oklahoma Geological Survey, 100 E. Boyd, Room N-131, Norman, OK 73019; (405) 325-3031 or (800) 330-3996, fax 325-7069.

Red Fork Workshop Scheduled for June

The Oklahoma Geological Survey, in cooperation with the Oklahoma City Geological Society, will sponsor a half-day workshop, "Fluvial-Dominated Deltaic Oil Reservoirs in Oklahoma: The Red Fork Play," on June 25 from 1 p.m. to 5 p.m. It will be held at the Home Builders Association of Greater Oklahoma, 625 West Interstate 44 Service Road, Oklahoma City. OGS geologist Rick Andrews is the primary presenter. To register, please contact the OCGS reservation lines at (405) 236-8086 or (405) 235-3648, ext. 40. If you have questions regarding the workshop, call Carol Jones at (405) 236-8086, ext. 11.

AAPG Annual Convention
Salt Lake City, Utah — May 17–20, 1998

During the past decade the petroleum industry underwent a revolution that is now paying dividends. It is not high prices or shortage of product that is fueling the petroleum industry today. For perhaps the first time in history, we are in the midst of economic success that is productivity driven! Advanced technology, new applications, and creative integration of disciplines are responsible for the industry's current prosperity and long-awaited rebound, hopefully making the current growth sustainable over the long term.

To maintain our productivity and efficiency, we geoscientists have to develop and share new ideas among ourselves and with our colleagues in other disciplines. And one of the best ways to keep up on the latest advances is at the AAPG annual meeting! The annual meeting is the key to the continued growth of our profession: hundreds of scientific presentations, hundreds of exhibitors with their latest technologies, career enhancement programs, and dozens of short courses, field trips, and prospect deals.

Utah is home to more natural arches and bridges than anywhere else on the globe. So what could be a better metaphor for the annual meeting than **Bridges to Discovery**—and a better logo than world-famous Rainbow Bridge?

The meeting will focus on investigating and understanding the bridges between geologists and engineers, between exploration and development, between science and policy, and not least, between today and the 21st century. And inclusion in the meeting of other professional organizations such as SPE, SEG, and SPWLA will foster **bridging disciplines** within and among geology, geophysics and engineering.

Technical sessions will emphasize **bridging technologies**, including new concepts in reservoir characterization, logging, petrophysics, and remote detection, among others.

Bridging continents and cultures will feature emerging exploration plays in every region of the world, expansion of the popular International Pavilion, and a special forum on dealings with indigenous peoples.

Utah and field geology are synonymous. Walk in the footsteps of John Wesley Powell and G. K. Gilbert to many of the best outcrop exposures you will ever see. The extensive field trip opportunities use world-class analogues to **build bridges to scientific discovery**.

In many ways, Salt Lake City is like the oil industry itself: born of the pioneer spirit, exciting, bold, booming, and just a little bit rough around the edges. We are proud to host you in 1998!

M. Lee Allison
General Chairman

Convention Agenda

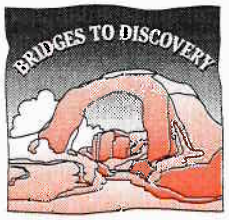

Technical Program

Monday, May 18

Quantifying Stratigraphy and Sedimentology for Reservoir Modeling
Future Trends in the International Petroleum Industry: Management
Carbonate Chemostratigraphy as a Chronostratigraphic, Paleoenvironmental, and Exploration Tool
New Exploration and Production Opportunities in Brazil and Venezuela
Faults: Seals or Migration Pathways?
Seismic Imaging—A Path to Improved Interpretation in Stratigraphic and Structural Settings
Selected Academic Research Topics
Modern and Ancient Lacustrine Depositional Systems
Future Trends in the International Petroleum Industry: Technology
Exploration and Production in Latin America
Impact Structures as Reservoirs and Exploration Targets
Reservoir Architecture of Fluvial-Deltaic Sandstones
Geochemical Evaluation of Hydrocarbons and Their Potential Sources in the CIS
Catastrophic Event Sedimentation: Storms vs. Tsunamis
Global Stratigraphic Correlation and Geochronology

Tuesday, May 19

Passive Margin, Deep-Marine Clastic Reservoirs
New Exploration and Production Opportunities in North America
Synsedimentary Tectonic Control of Sequence Stratigraphy: Concepts and Compressional Settings
Exploration and Production in Australasia
New Concepts in Reservoir Characterization, Modeling, and Simulation
Optimization and Growth of the Independent Professional Geological Practice
Coalbed Methane Characterization, Development, and Trends
Modern and Ancient Carbonate Eolianites
Synsedimentary Tectonic Control of Sequence Stratigraphy: Extensional Settings
Exploration and Production in Africa and the Middle East
Exploration and Development of Carbonate Reservoirs—3-D Seismic and Horizontal Drilling
Evaluation of Trap Style and Integrity
Environmental Issues of Petroleum Operations in the CIS
Resolution of Environmental Issues of Offshore Petroleum Operations
Marine Ichnology and Taphonomy
Siliciclastic Sedimentology and Stratigraphy

Wednesday, May 20

Fractured Petroleum and Geothermal Reservoirs
Mixed Carbonate and Siliciclastic Depositional Environments
Cretaceous of the Western Continental Interior: From Basin to Pore
Exploration and Production in Eastern and Central Eurasia
Quantitative Aspects of Petroleum Systems: Global Case Studies
Hydrocarbons in Overthrust Belts

3-D and Time-Lapse Reservoir Characterization
Paleoclimatic Indicators and Climatic Modeling
International Geothermal Development—Business and Resource Potential
Applications of NMR Logging in Exploration and Production
Predictive Quality of Reservoir Characterization and Simulation: Global Case Studies
Petroleum Geology
4-D Modeling and Animation
Advances in Geostatistics

Short Courses

Planning and Design Considerations for Horizontal Well Technology, *May 16–17*
Rock Mechanics for Reservoir Exploitation, *May 16*
Understanding Fluvial Reservoirs, *May 16–17*
Evaluating Reservoirs, Seals, and Pay, *May 16–17*
Quick Look Mapping Techniques for Prospect Evaluation, *May 16–17*
Natural Attenuation for Remediation of Contaminated Sites, *May 15–16*
The Geologist as Entrepreneur, *May 17*
The Internet Explored for the Petroleum Professional, *May 16*
Estimating the Gas-in-Place in a Coal Natural Gas Reservoir, *May 16–17*
Modern and Ancient Deep-Sea Fan Sedimentation, *May 15–17*
Tectonics of Sedimentary Basins, *May 16–17*
Radiogenic and Stable Isotopes in Chronostratigraphic, Paleoenvironmental, and Basin Analysis, *May 16–17*
Tidal Rhythmites and Their Applications and Implications—A Core Workshop, *May 17*
Advanced Surface Geochemical Methods and Interpretation Integrated with Geological and Geophysical Case Histories, *May 16*
Core and Reservoir Modeling Workshop: Fluvial-Deltaic Nearshore Sands of the Ferron Sandstone, *May 17*
Underbalanced Drilling Solutions for Improved Reservoir Exploration, *May 21–23*
Hydrogeology of Sedimentary Basins with Application to Hydrocarbon Exploration, *May 21–22*
Practical Geostatistics and Reservoir Characteristics, *May 22–23*
Current Technology and Processes, *May 21–23*
An Introduction to Decision Analysis and Value of Information for Exploration Projects, *May 21–22*
Assigning Petrophysical Properties to Fault Zones, *May 21–22*
Desktop GIS: A Data Synthesizing and Analysis Tool for the Natural Resource Exploration and Extraction Industries, *May 21*
Borehole and Core NMR and Other Views of Permeability, *May 21*
Seismic Velocity Model Building, *May 21*

Field Trips

Stratigraphy and Structure of the Sevier Thrust Belt and Proximal Foreland-Basin System in Utah: A Transect from the Sevier Desert to the Wasatch Plateau, *May 13–16*
Sequence Stratigraphy, Stratal Patterns, and Structure—and Much More—of the Eastern Uinta Mountains, Utah, *May 14–17*
Modern Lacustrine Environments, Lake Bonneville—Great Salt Lake, Utah, *May 14–16*
Controls on Mixed Carbonate-Siliciclastic Stratigraphic Architecture: Pennsylvanian Holder Formation, Sacramento Mountains, New Mexico, *May 14–16*

The Charleston-Nebo Allochthon: Missing Link of the Sevier Belt, *May 16*
Geology of the Great Salt Lake and Antelope Island, Utah, *May 16*
Geology along the Wasatch Front, *May 16*
Successful and Cost-Effective Solutions to Remediation of Petroleum-Contaminated Soil and Ground Water, *May 16*
Facies and Fracture Architecture of the Tensleep Sandstone, Bighorn Mountains, Wyoming, *May 14–16*
Permian-Triassic Deposystems, Paleogeography, Paleoclimate, and Hydrocarbon Resources in Canyonlands and Monument Valley, Southeastern Utah, *May 13–17*
Sequence Stratigraphy and Facies Distribution, Pennsylvanian Algal Mounds, Paradox Basin, Utah, *May 14–16*
Concepts and Practical Applications of Sequence Stratigraphy in Shallow Marine and Coastal Plain Successions, Book Cliffs, Utah, *May 13–16*
Hydrocarbon Habitat and Special Geologic Problems of the Great Basin, *May 14–16*
Jurassic Morrison Dinosaurs of Utah and Colorado, *May 14–16*
Stratigraphic Framework for Reservoir Modeling in Fluvial-Deltaic Deposits: A Para-sequence Level Analysis and Reservoir Characterization of the Ferron Sandstone, Utah, *May 14–16*
Late Cretaceous Facies Tract, Book Cliffs Area and Ferron Deltaic Complex, Utah, student chapter trip (restricted to students and faculty advisors only), *May 16–17*
High-Resolution Stratigraphy of the Green River Formation, Raven Ridge, Northeast Uinta Basin: Facies, Cycle Stacking Patterns, and Petroleum Subsystems in a High-Gradient, High-Energy Lacustrine System, *May 20–23*
Salt and Extensional Tectonics in the Northern Paradox Basin, Southeastern Utah, *May 21–24*
Classic Geology of Zion and Bryce Canyon National Parks and the Grand Staircase–Escalante National Monument, Utah, *May 21–23*
Grand Canyon Geology via the Colorado River, Arizona, *May 21–29*
Coalbed Methane Operations and Coal Basin Geology: San Juan Basin, New Mexico and Colorado, *May 21–24*
Geothermal Resources of Utah, *May 21–22*
Stratigraphy, Structure, and Source Rock Potential of Ordovician to Devonian Rocks of Roberts Mountains Allochthon, Central Nevada, *May 20–23*
Coupled Structure and Sedimentation through 100 Million Years of Thrust Wedge Evolution, Sevier Thrust Belt, Northern Utah and Western Wyoming, *May 21–23*
Sedimentology and Sequence Stratigraphic Architecture of Upper Cretaceous Mesaverde Group, Southwest Wyoming, *May 20–23*
Cambrian Paleoecology and Sequence Stratigraphy in the Eastern Great Basin, *May 20–22*
Devonian, Mississippian, and Pennsylvanian-Permian Organic Buildups and Mudmounds of Idaho, *May 21–23*

AMERICAN ASSOCIATION OF PETROLEUM GEOLOGISTS
AAPG
1917

For more information about the annual meeting, contact AAPG Annual Convention, P.O. Box 979, Tulsa, OK 74101-0979; phone (918) 560-2617, fax 918-560-2684 or 800-281-2283; World Wide Web: www.geobyte.com/meetings.html

Oklahoma ABSTRACTS

The Oklahoma Geological Survey thanks the American Association of Petroleum Geologists, the Geological Society of America, and Elsevier Science Ltd. for permission to reprint the following abstracts of interest to Oklahoma geologists.

The AVO Response of a Pennsylvanian Age Channel Sandstone in the Arkoma Basin, Oklahoma

ERIC KUBERA, ROGER A. YOUNG, and *ALAN LEAVER,* School of Geology and Geophysics, University of Oklahoma, Norman, OK 73019

A seismic line imaging a gas-producing channel sand in the Pennsylvanian Hartshorne Formation was acquired in September 1994. The dataset was processed to retain relative amplitude fidelity and has been analyzed for anomalous amplitude behavior. Frequency domain filtering and CMP mixing were applied to improve the signal/noise ratio of the data. Despite this improvement, visual inspection of amplitude variations on trace gathers was not possible. Statistical determination of several amplitude attributes, however, provided an alternative procedure for interpretation of amplitudes. Attribute plots show that the channel sand does, indeed, have a distinctive AVO response. This signature is a positive normal incidence reflection of moderate relative amplitude which displays a strong increase in amplitude with offset.

Reprinted as published in the American Association of Petroleum Geologists *Bulletin*, v. 81, p. 1352, August 1997.

Three-Dimensional Seismic Interpretation from the Triangle Zone of the Frontal Ouachita Mountains and Arkoma Basin, Pittsburg County, Oklahoma

M. H. VALDERRAMA, K. C. NIELSEN, and *G. A. McMECHAN,* University of Texas at Dallas, P.O Box 830688, Richardson, TX 75083

Analysis of 28.5 km^2 of three-dimensional (3-D) seismic reflection data from the triangle zone of the Ouachita fold-and-thrust belt and the foreland Arkoma basin reveals structural details not recognized previously in conventional two-dimensional (2-D) seismic data. The data indicate that the frontal Kiowa syncline in the Arkoma basin has been passively uplifted by blind thrusting at the Morrowan Wapanucka Limestone level, and that smaller wavelength folds are produced by thrusting at shallower levels in the Atoka Formation. Faulting at deeper levels in the Hunton and Arbuckle groups has been traditionally interpreted as normal, but our analysis of this data set indicates that, in this area, normal faults were reactivated during the Ouachita orogeny as reverse faults, and the changes in fault separation can be followed along strike. These faults show the same trend as the overlying thrusts and are normal or have minor inversion where the overlying thrusts have small displacement. These faults have been completely inverted where the overlying thrusts have more displacement, suggesting a genetic relation between the Wapanucka thrusts and the inversion of the Hunton and Arbuckle faults.

Four reflections were chosen for analysis: one reflection in the lower Atoka Formation, two reflections repeated in the Wapanucka Limestone, and a fourth reflection in

the Hunton Group. All of these surfaces exhibit the same geometry with the fold axes plunging to the southwest. Variations in bearing and plunge of fold axes in the Wapanucka Limestone can be directly correlated to changes in displacement and ramp height along strike. The similarity between surface geometries suggests that the last deformation took place at deeper levels in the Hunton and Arbuckle groups and folded the overlying thrusts. Reactivation of Atokan normal faults at deeper levels in the Arkoma basin and Ouachita subthrust play may be more widespread than previously recognized.

Reprinted as published in the American Association of Petroleum Geologists *Bulletin*, v. 80, p. 1185, August 1996.

Structural Geometry of Thrust Faults in the Red Oak and Talihina Quadrangles, Latimer and Le Flore Counties, Arkoma Basin, Southeastern Oklahoma

SYED MEHDI and *IBRAHIM CEMEN*, School of Geology, Oklahoma State University, Stillwater, OK 74078

The Arkoma basin and the Ouachita Mountains of southeastern Oklahoma and western Arkansas were formed during the late Paleozoic Ouachita orogeny. The Choctaw fault forms the boundary between the frontal Ouachitas, characterized by imbricated thrust faults with tight to overturned folds, and the Arkoma basin, which is marked by gentle folds with minor faulting, due to mild compressions. To delineate the structural geometry of the Late Paleozoic thrust faults in Talihina and Red Oak quadrangles, six balanced structural cross-sections were constructed based on surface geologic maps by Oklahoma Geological Survey, wire line log data, scout tickets and reflection seismic lines donated by EXXON and AMOCO oil companies.

The Pine Mountain, Ti Valley and other thrust faults exposed at the hanging wall of the Choctaw fault zone are interpreted in the cross-sections as imbricate fans splaying from the Choctaw detachment surface. The structural cross-sections suggest the presence of a well-defined duplex structure containing at least two horse structures in the footwall of the Choctaw fault zone. The Springer detachment is the floor thrust and the Lower Atokan Detachment is the roof thrust of the duplex structure. A well-defined triangle zone is also observed in the footwall of the Choctaw fault zone. It is bounded by the subsurface continuation of the Carbon fault on the north as a blind backthrust, and the Choctaw fault on the south. The triangle zone is floored by the Lower Atokan Detachment.

Reprinted as published in the Geological Society of America *1998 Abstracts with Programs*, v. 30, no. 3, p. 11–12.

Triangle Zone Geometry of the Frontal Ouachitas in the Wilburton Area, Arkoma Basin, Oklahoma: Implications for Fault Sealing in the Wilburton Gas Field

IBRAHIM CEMEN, ZUHAIR AL-SHAIEB, ATA SAGNAK, RODNEY FELLER, and *SALEEM AKTHAR*, School of Geology, Oklahoma State University, Stillwater, OK 74078

The Wilburton gas field, situated in the central part of the Arkoma basin, produces mainly from the lower Atokan Spiro Sandstone. In the Wilburton area, we constructed seven balanced structural cross sections, prepared a top structure contour map of the Spiro Sandstone and developed pressure-depth profiles for the Spiro reservoirs.

The cross-sections suggest the presence of a well developed triangle zone between the mildly compressed Arkoma basin and frontal Ouachitas fold-thrust belt. This zone is floored by the Lower Atokan detachment and flanked by the Choctaw fault to the south and the Carbon fault to the north. The south-dipping Choctaw fault contains several south-dipping imbricate fan thrust faults in its hanging wall. The footwall of the Choctaw fault contains several duplex structures formed by hinterland dipping imbricate thrust faults, splaying in a break-forward sequence of thrusting from the Springer detachment (floor thrust). The duplexes join to the Lower Atokan detachment (roof thrust) in the Atoka Formation. The Lower Atokan detachment continues in the Atoka Formation northward and displaces the Red Oak Sandstone before reaching a shallower depth and forming the Carbon fault as a north-dipping backthrust below the San Bois syncline. When restored to their position at the time of the Spiro deposition by using the key-bed restoration method, the cross-sections indicate about 60% shortening in the Wilburton area.

In the duplex structures, the Spiro reservoirs that were brought to structurally higher positions by the thrust faults generally exhibit higher pressure-depth gradients. Therefore, we suggest that the thrusting in the Wilburton area was formed after the Spiro Sandstone reservoirs were charged, and the duplex structures might have provided seals for the reservoirs. The top Spiro structure contour map suggests that the duplexes are separated by tear faults which may have served as lateral seals.

Reprinted as published in the American Association of Petroleum Geologists *1997 Annual Convention Official Program*, v. 6, p. A19.

How Well Do We Know the Natural Gas Resource Potential of the Arkoma Basin in Arkansas and Oklahoma?

BRIAN W. HORN, Amoco Production Co., Denver, CO; *THOMAS J. WOODS*, Ziff Energy Group Ltd., Houston, TX; and *JOHN B. CURTIS*, Colorado School of Mines, Golden, CO

Current estimates for the ultimate recovery of natural gas in the Arkoma basin are in the range of 13–15 Tcf, of which approximately 4.5 Tcf are remaining proved reserves. Recent studies by the Potential Gas Committee and the US Geological Survey have concluded that an additional 2–4 Tcf exists as the potential resource for a total of 16–18 Tcf as the ultimate recoverable resource. However, analysis of field size distributions and production data suggests that 34–38 Tcf is a more reasonable estimate of the ultimate recoverable resource, which implies a remaining potential resource of 20–24 Tcf for the Arkoma basin.

The current size range of producing gas fields in the basin shows a bimodal distribution centered around class 8 (0.5–3.1 Bcf) and class 12 (8–50 Bcf) field sizes. If an exponential distribution is assumed for the basin's ultimate recoverable resource, a distribution normalized on a class 12 field size yields an estimate of 20–24 Tcf as the remaining recoverable resource. This estimate is corroborated by analyzing historical production and completion trends for the basin and extrapolation of reserve additions over the next 10–20 years. These data suggest that 4–5 Tcf could be added to the existing reserve base within the next ten years and indicate significant potential of this previously unrecognized resource. Separation of the historical production data into discrete depth intervals yields a better understanding of current producing trends by formation, structural configuration and reservoir quality through time. Integration of these data into a regional geologic context allows a high-resolution prediction of the ultimate resource potential and forms the basis for evaluating areas of future exploration.

Reprinted as published in the American Association of Petroleum Geologists *Bulletin*, v. 82, p. 526, March 1998.

The Role of Genetic Stratigraphy in Reservoir Characterization of Mixed Siliciclastic/Carbonate Valley-Fill Reservoirs: Example from the Pennsylvanian Wapanucka Limestone and Spiro Sandstone, Arkoma Basin, Southeastern Oklahoma

BRIAN W. HORN, Amoco Production Company, Denver, CO

The Wapanucka Limestone and Spiro sandstone comprise a (3rd order) genetic sequence bounded by deposits and surfaces that record marine deepening. This final stage of passive-margin deposition contains two smaller scale (4th order) mixed carbonate-siliciclastic cycles that record progradation (highstand system tract), valley incisement (lowstand systems tract), valley filling and transgression (transgressive systems tract). Reservoir development within these smaller scale cycles show systematic lateral and vertical variation and compartmentalization that can be attributed to their stratigraphic position within the larger stratigraphic cycle.

Core analysis and regional mapping demonstrates the presence of a 4th order regional erosion surface (sequence boundary) which incised 10–60 feet into the underlying Wapanucka shelf carbonate cycles. Progradation of the seaward-stepping clastic sub-Spiro shoreface (HST) created laterally continuous and interconnected reservoirs that are locally truncated by younger "Foster" paleovalleys with 60–140 feet of relief, juxtaposing fluvial-estuarine sandstones and Wapanucka shelf carbonates.

In each of the systems tracts, these 4th order cycles show systematic variation in reservoir quality, thickness and compartmentalization that may be related to their position within the larger genetic sequence. Shelf carbonate facies are primarily a non-reservoir unit, whereas the regressive clastic shoreface cycles are productive in the northern part of the basin. While both valley fills contain reservoir quality sandstones, the older Wapanucka valley-fill sandstones form isolated reservoir units in the northern part of the basin. Younger "Foster" valley-fill reservoirs, found across the entire basin, are thicker, contain little carbonate skeletal material and have larger areas of drainage. Comparison of these two valley-fills show differences in reservoir quality, architecture and compartmentalization that can be understood from the context of the stratigraphic position within a stratigraphic hierarchy.

Reprinted as published in the American Association of Petroleum Geologists *1997 Annual Convention Official Program*, v. 6, p. A53.

Numerical Modeling of Heat Flow in the Arkoma Basin

PEIZHONG WANG, Dept. of Geology, George Washington University, Washington, DC

The Arkoma Basin is an E-W–trending foreland basin that formed in response to the late Paleozoic Quachita orogeny (Thomas, 1985) and is an excellent example of prolific natural gas production from strata considered to be overmature (R_o>3.0). An expected northerly trend for thermal gradient and fluid expulsion through Cambrian sandstones, related to south-to-north basin closure, was recognized by Bethke et al. (1988). However, there is an unexpected, eastward component to increasing thermal maturity in Carboniferous strata (Houseknecht et al., 1987). This trend cannot be explained by sedimentary or tectonic burial depth, nor by the presence of igneous intrusions. Houseknecht et al. (1987) hypothesized that the faces distribution and orientation of regional faults, in combination with loading or overpressuring, would induce upward and eastward fluid flow through the foreland basin. Transfer of heat from the deep ba-

sin by this mechanism could potentially explain not only the high overall thermal maturity of the basin but also the trend of increasing R_o values to the east.

The purpose of this study is to explore whether east-west facies changes or similarly oriented structures (including faults, folds, cleavages, and fractures) could act as conduits to bring hot basinal fluids into shallow depths.

The majority of the work will involve using the two dimensional numerical code Basin2 (Bethke, 1985; Bethke et al., 1993; Hayba and Bethke, 1995) to simulate the heatflow through the basin. This code accounts for conductive and convective transport of heat in response to basin loading.

In conclusion, this study will improve our understanding of the thermal evolution of the Arkoma basin as well as the mechanisms of hydrocarbon preservation under conditions of high thermal maturity.

Reprinted as published in the American Association of Petroleum Geologists *Bulletin*, v. 81, p. 1783, October 1997.

Magnetotelluric Study of the Arkoma Basin and Ouachita Mountains, Southeastern Oklahoma

KEVIN MICKUS, Dept. of Geosciences, Southwest Missouri State University, Springfield, MO 65804

Seventy magnetotelluric stations collected in three regional profiles in southeastern Oklahoma were analyzed to determine the region's electrical resistivity structure. These profiles, which extend from Atoka, Oklahoma, to the Texas/Oklahoma border, cross the tectonic provinces of the Arkoma foreland basin, Ouachita frontal zone and the Broken Bow uplift, which are associated with the Ouachita orogeny. The majority of the stations recorded data in the frequency range from 0.005 Hz to 100 Hz, which samples electrical resistivity variations within the crust. The data were processed into the transverse electrical and magnetic (TE and TM) modes and the TM mode data were used to construct a series of one- and two-dimensional crustal electrical resistivity models. These models, constrained by electrical resistivity well logs, indicate that several units, including the Atoka Formation (20–50 ohm-m), Stanley Group (20–120 ohm-m), Arbuckle Group (500–2000 ohm-m), Womble Formation (10–20 ohm-m), Wapanucka Limestone (50–200 ohm-m) and the Coastal Plain sediments (10–20 ohm-m) were resolvable. Two-dimensional models along profile one indicate that the southwestward extension of the Broken Bow Uplift may be present along the Texas/Oklahoma border. These models also indicate that the depth to the Arbuckle Group ranges from 3–4 km in the Arkoma Basin to nearly 9 km near the Texas/Oklahoma border. Wide station spacing limited the resolution of determining the subsurface location of thrust and normal faults but the Ti Valley thrust fault is resolvable on all three profiles.

Reprinted as published in the Geological Society of America *1997 Abstracts with Programs*, v. 29, no. 2, p. 40.

Depositional Systems and Sequence Stratigraphy of the Spiro Sandstone Interval, Arkoma Basin of Eastern Oklahoma

ARTHUR W. CLEAVES, School of Geology, 105 Noble Research Center, Oklahoma State University, Stillwater, OK 74078

The basal Atokan Spiro Sandstone Interval of eastern Oklahoma was deposited as an assemblage of marine shelf, wave-dominated deltaic, incised valley-fill channel, tidal flat, and estuarine environments during a eustatic cycle involving large-scale marine

regression followed by a lengthy period of marine transgression. Spiro Interval sedimentation began with high-stand deposition of prodelta shale fed onto the Wapanucka distally steepened ramp by earliest Atokan deltas located in the Fort Smith area. This was followed by eustatic regression that brought about fluvial downcutting into the "pre-Spiro shale" by several channel complexes, collectively termed the Foster channels, that transported coarse-grained siliciclastics from a northerly, cratonic source to lowstand, perched deltas present along the ramp's outer margin.

The subsequent transgression involved both a eustatic rise in sea level and tectonic collapse of the ramp margin, indicating a change from a passive continental margin to collisional plate boundary. Terrestrial strandplain facies of the lowstand deltas were reworked westward parallel to strike along the middle shelf, while the Foster channel incised valleys backfilled with bayhead delta lobes, estuarine deposits, tidal flats, and lastly, bioturbated, inner-shelf marine sediment. Several temporary stillstands allowed local bayhead deltas to spill out onto the middle and inner shelf. Complete collapse of the ramp resulted in the deposition of crinoid-rich sheet sandstone across underlying valley-fill and delta-plain facies and ultimately brought about the retreat of deltaic sedimentation to a new shelf margin more than forty miles to the north.

Reprinted as published in the American Association of Petroleum Geologists *Bulletin*, v. 81, p. 1348–1349, August 1997.

Sequence Stratigraphy of the Basal Atokan Spiro Sandstone Interval, Arkoma Basin of Oklahoma

ARTHUR W. CLEAVES and *ZUHAIR AL-SHAIEB*, School of Geology, Oklahoma State University, 105 Noble Research Center, Stillwater, OK 74078

The lowermost Atokan Spiro Sandstone Interval of eastern Oklahoma between Fort Smith and McAlester accumulated in deltaic, incised-valley fluvial, estuarine, and open marine shelf environments on the southern, passive margin of the early Pennsylvanian North American continent. Within the Spiro, the overall vertical facies succession records one cycle of regression and transgression that was generated by the combined effects of tectonics and glacial eustasy. This interval is directly underlain by Wapanucka distally steepened ramp carbonates. An older cycle of deltaic progradation and ramp sedimentation is seen with the subjacent Cromwell/Union Valley Interval. The Spiro itself, in turn, underlies a thick section of deep water Early and Middle Atokan submarine fan and abyssal basin deposits which were laid down beyond the newly foundered shelf margin. Spiro Interval sedimentation began with highstand deposition of prodelta shale on top of the Wapanucka across the eastern two-thirds of the ramp. Eustatic regression brought about fluvial incision of the "pre-Spiro Shale" unit and transported pebble-sized quartz out onto the shelf from a northern, continental interior source. These Foster Channels supplied sand to lowstand, perched, wave-dominated deltas centered in western Le Flore County. With the ensuing transgression, the upper part of the deltaic sand bodies were reworked parallel to strike (westward) on the outer shelf, while the incised valleys backfilled with estuarine, bayhead deltaic, and inner-shelf marine sediment. Several temporary stillstands allowed for the "spillout" of local bayhead deltas from their valleys onto the middle and inner shelf. Complete submergence brought about reworking of the sediments in the estuarine deltas and adjacent high-energy shoreface environment to form the crinoid-rich sheet sand present across the top of the entire coarse-grained Spiro unit.

Reprinted as published in the Geological Society of America *1996 Abstracts with Programs*, v. 28, no. 7, p. A-367.

Continental-Scale Allocyclic Controls on the Lithostratigraphy of a Middle Pennsylvanian Cyclothem

C. BLAINE CECIL, FRANK T. DULONG, BRUCE WARDLAW, and *N. TERENCE EDGAR,* U.S. Geological Survey, Reston, VA; and *RONALD WEST,* Kansas State University, Manhattan, KS

To evaluate allocyclic controls on the lithostratigraphy of Pennsylvanian cyclothems, we conducted a continental-scale correlation of strata resulting from a single Middle Pennsylvanian sea-level cycle. The interval evaluated is a probable parasequence resulting from a fourth-order sea level cycle.

Mineral paleosols that bound the cycle can be correlated across the United States. The paleosol types document paleolatitudinal climate gradients from very wet rainforest conditions in the east (Paleo-Ultisols, to seasonal rainfall conditions in the mid-continent (Paleo-Vertisols), to semiarid or arid conditions in the west (Paleo-Aridisols and microkarst exposure surfaces with pedogenic-breccias on marine carbonates).

From central Kansas eastward, the mineral paleosols are unconformably overlain by coal, a paleo-Histosol. Coal beds document a rise in water table driven by rising sea-level, increased rainfall, or both. The unconformable contact between the mineral and organic paleosols marks the parasequence boundary.

From eastern United States through the mid-continent, sea level rise was accompanied by a dramatic increase in siliciclastic influx. Carbonate deposition dominated western basins. As sea level continued to rise, siliciclastic deposition ceased and carbonate deposition dominated, except in eastern-most outcrops. A paleosol marks the top of the cycle. The cyclic variation in sediment supply was climatically controlled as patterns in the amount and seasonality of rainfall changed both temporally and spatially. Tectonics effected accommodation space in the Arkoma, Fort Worth, and Paradox basins, but, because the interval thickness changed little, it had little or no effect on sediment supply at the time scale of one sea level cycle.

Reprinted as published in the American Association of Petroleum Geologists *1997 Annual Convention Official Program,* v. 6, p. A19.

Sediment Accommodation Regions: Fragmentation of a Subsiding Shelf

W. LYNN WATNEY, JOHN C. DAVIS, and *JOSEPH M. KRUGER,* Kansas Geological Survey, Lawrence, KS; and *JAN HARFF,* Baltic Sea Research Institute, Rostock, Germany

Spatial analysis of isopach, structure, and lithofacies data, including shelf-wide mapping of Upper Pennsylvanian cyclothem-scale genetic stratigraphic units (GSUs) and genetic sets (GSs), provides consistent delineation of distinctive kilometer-scale sediment accommodation regions (SARs), in the form of rhombic and arcuate shaped subdivisions of the 100,000 km^2 shelf bordering the Anadarko and Arkoma basins. Basinward trends of increasing sediment accommodation space are interrupted by areas of seemingly episodic structural movements that define the SARs. The regions closely correspond to heterogeneous crustal blocks defined by potential field geophysics, basement geology and geochronology. Episodic structural activity along boundaries of SARs may have resulted from changes in strength and orientation of far-field stresses associated with the Ouachita orogeny.

Comparison of stratal and sedimentation patterns suggest that differing elevations of SARs led to contrasting relative sea-level histories during periods of widely fluctuating,

Rotational Reflectance of Dispersed Vitrinite from the Arkoma Basin

DAVID W. HOUSEKNECHT, U.S. Geological Survey, 915 National Center, Reston, VA 20192; and *CHRISTOPHER M. B. WEESNER,* Booz-Allen and Hamilton, 300 Convent St., San Antonio, TX 78205

Rotational reflectance of dispersed vitrinite provides superior documentation of thermal maturity and a capability for interpreting relative timing between thermal and kinematic events in Arkoma Basin strata characterized by vitrinite reflectances up to 5%. Rotational reflectance (R_{rot}) is a more precise and less ambiguous index of thermal maturity than maximum (R'_{max}), minimum (R'_{min}), and random (R_{ran}) reflectance. Vitrinite reflectance anisotropy becomes sufficiently large to be measurable (using a microscope equipped with an automated rotating polarizer) at ≈2% R_{rot} and increases following a power function with increasing thermal maturity.

Rotational reflectance data can be used to infer the shape of the vitrinite reflectance indicating surface (i.e., indicatrix) and, in turn, to enhance interpretations of the timing between thermal maxima and compressional tectonic events. Data from three wells in the Arkoma Basin–Ouachita frontal thrust belt are used as examples. The absence of offsets in measured R_{rot} across thrust faults combined with a predominance of uniaxial vitri-nite in the thrust faulted part of the section suggest thermal maximum post-dated thrust faulting in the western Ouachita frontal thrust belt of Oklahoma. In contrast, the general absence of offsets in measured R_{rot} across thrust faults combined with a predominance of biaxial vitrinite in the thrust faulted part of the section suggests that the thermal maximum was coeval with thrust faulting in the eastern Ouachita frontal thrust belt of Arkansas. The presence of biaxial vitrinite in an allochthonous section and uniaxial vitrinite in an underlying, autochthonous section suggests that the thermal maximum was coeval with listric thrust faulting in the central Arkoma Basin of Oklahoma, and that rotational reflectance data can be used as a strain indicator to detect subtle decollement zones.

Reprinted as published in *Organic Geochemistry*, v. 26, no. 3/4, p. 191.

Coal Geology of Eastern Oklahoma—An Overview

LEROY A. HEMISH, Oklahoma Geological Survey, 100 E. Boyd, Room N-131, Norman, OK 73019

Oklahoma's commercial coal deposits are located in the eastern part of the state, within the Western Interior Region of the Interior Coal Province of the conterminous United States. They occur in an area of some 8,000 square miles in strata of Desmoinesian (Middle Pennsylvanian) age. The coal beds occur in two structurally different areas—the northeast Oklahoma shelf area, where beds dip west-northwest ½° to 2°, away from the Ozark uplift; and the Arkoma basin area, where beds crop out along the sides of eroded, faulted, anticlines and synclines, with dips ranging from 3° to nearly vertical.

A total of 25 named bituminous coal beds are present and have been mined in eastern Oklahoma. About 41% of the coal is low- and medium-volatile in rank and occurs in the eastern part of the Arkoma basin; in the western part of the basin the coal is mostly high-volatile C in rank; and in the remaining coal-bearing counties the coal is mostly high-volatile A and B in rank.

Identified coal resources of Oklahoma total about 8 billion short tons, of which 1,590 million tons is classified as reserves. Coal beds in the shelf area average about 2.0 ft thick, and in the basin area, 1 to 10 ft thick. Of the remaining resources 76% are in the

Arkoma basin and 24% are in the shelf area.

Records of coal production in Oklahoma have been kept since 1873. Graphs show that production peaks are related to World War I, World War II, and the Arab Oil Embargo. In the early history of mining, coal was produced almost exclusively from underground mines. Through time, development of new techniques, availability of modern heavy equipment, and consideration of safety factors led to a change in mining methods. Today, almost all coal is mined in surface mines. Oklahoma's production peaked in 1981, when about 5.76 million tons was produced from 51 mines. In 1995 about 1.873 million tons was produced from 17 mines.

Reprinted as published in the Geological Society of America *1997 Abstracts with Programs*, v. 29, no. 2, p. 14.

Coal Geology of McIntosh and Muskogee Counties, Oklahoma

LEROY A. HEMISH, Oklahoma Geological Survey, 100 E. Boyd, Room N-131, Norman, OK 73019

McIntosh and Muskogee Counties are located in the east-central part of the coal belt of eastern Oklahoma. Coal-bearing strata of Desmoinesian (Middle Pennsylvanian) age underlie nearly all of McIntosh County and ~500 mi^2 in the western two-thirds of Muskogee County. Prior to the investigations by the Oklahoma Geological Survey in recent years, the coal geology of the two-county area has been poorly understood.

In McIntosh County eight coal beds have been shown to have commercial potential: Stigler (McAlester Formation); Rowe (Savanna Formation); Lower Witteville, Secor, Peters Chapel (new name), and Wainwright (Boggy Formation); and Mineral and Croweburg (Senora Formation). Remaining resources of coal in the county total 36,319,000 short tons, and reserves total 5,437,000 short tons.

In Muskogee County ten coal beds have been shown to have commercial potential: Hartshorne (Hartshorne Formation); Keefton (new name) and Stigler (McAlester Formation); Spaniard and Rowe (Savanna Formation); Secor, Peters Chapel, and Wainwright (Boggy Formation); and Tebo and Croweburg (Senora Formation). Remaining resources in the county total 95,557,000 short tons, and reserves total 11,141,000 short tons.

Coals of the two-county area are predominantly of high-volatile A bituminous (hvAb) rank. In Muskogee County the Hartshorne, Keefton, and Secor coals have much lower sulfur contents than the others, averaging ~1.1%. In McIntosh County the Secor coal has the lowest sulfur content, averaging ~2.5%. The combined average sulfur content of all the other coals in the two counties averages ~5%.

In the past coal has been mined by both underground and surface methods in the area. No coal is being produced in either county at the present time.

Reprinted as published in the American Association of Petroleum Geologists *Bulletin*, v. 81, p. 1351, August 1997.

Oklahoma Coal Database

BRIAN J. CARDOTT, Oklahoma Geological Survey, 100 E. Boyd, Room N-131, Norman, OK 73019

Since 1984, the Oklahoma Geological Survey (OGS) has been developing a computerized GIS-based (geographic information system) database of information (location, quantity, and quality) on Oklahoma's coal resources, as part of the National Coal Resources Data System (NCRDS). The NCRDS, initiated in 1975, is a cooperative program of the U.S. Geological Survey and state geological surveys of coal-producing states.

Geologists of the OGS collected stratigraphic and analytical data from every available source, including field investigations (mine and outcrop), coal-mining companies, State and Federal agencies, well drillers, the OGS drilling program, individuals, and literature search. The database presently includes data from 12 counties (Craig, Creek, Mayes, McIntosh, Muskogee, Nowata, Okfuskee, Okmulgee, Rogers, Tulsa, Wagoner, and Washington) in the northeast Oklahoma shelf area.

Stratigraphic header and data tables contain 20,775 records of stratigraphic and geologic information from 4,457 locations.

Analytical header and data tables contain location, stratigraphic and geologic information, determined rank, and analytical (chemical and petrographic) data of 545 samples.

A production table lists Oklahoma coal production by county, percentage surface mined, and value from 1908 to the present.

Examples of queries, maps, and graphs, generated from the data, will be presented.

Reprinted as published in the American Association of Petroleum Geologists *Bulletin*, v. 81, p. 1348, August 1997.

Coal-Bed Methane Resources and Reserves of Osage County, Oklahoma

SAMUEL A. FRIEDMAN, Oklahoma Geological Survey, 100 E. Boyd, Room N-131, Norman, OK 73019

About 100 oil wells have been recompleted in and are producing gas from four Middle Pennsylvanian bituminous coal beds, 1,200–1,700 feet deep in eastern Osage County since January 1, 1995. The present study applied the standard method of reliability to determine coal resources, and thence coal gas resources from geophysical logs in this county. Cored coal samples and coal-test well data were not available for accurate resource determination. The geophysical logs were not originally set up to detect coal, let alone thin coal beds one to three feet thick, thus making coal-bed thickness interpretation a hazardous procedure with great potential for major errors in coal resource determination and subsequently in coal-bed methane resource determination.

To avoid the high likelihood of exaggerated quantities of coal resources, the author restricted the total area to seven and one-half townships, the number of coals to three per well in five of these townships, and to two per well in two and one-half townships. All coal-beds were assumed to be only one foot thick and to contain only 150 cubic feet of gas per ton of coal.

Thus a minimum of 553 million tons of coal resources and 83 billion cubic feet of coal-bed methane resources are estimated to be present in eastern Osage County, Oklahoma.

At a 50% recoverability factor, there are 41 billion cubic feet of coal-bed methane reserves present.

Reprinted as published in the American Association of Petroleum Geologists *Bulletin*, v. 81, p. 1350, August 1997.